

Redox Chemistry of the Triplet Complex (PNP)Co<sup>I</sup>

Michael J. Ingleson, Maren Pink, Hongjun Fan, and Kenneth G. Caulton\*

Department of Chemistry, Indiana University, Bloomington, Indiana 47405

Received July 6, 2007; E-mail: caulton@indiana.edu

**Abstract:** Reaction of PNPCo, where PNP is (tBu<sub>2</sub>PCH<sub>2</sub>SiMe<sub>2</sub>)<sub>2</sub>N<sup>−</sup>, with the persistent radical galvinoxyl, G, gives PNPCo<sup>I</sup>G, a nonplanar S = 3/2 species. Reaction with PhCH<sub>2</sub>Cl or with 0.5 mol I<sub>2</sub> gives PNPCoX (X = Cl or I, respectively), but additional I<sub>2</sub>, seeking Co<sup>III</sup>, gives instead oxidation at phosphorus: (tBu<sub>2</sub>P(I)CH<sub>2</sub>SiMe<sub>2</sub>NSiMe<sub>2</sub>CH<sub>2</sub>P(tBu<sub>2</sub>)Co)<sub>2</sub>. Hydrogen-atom transfer reagents fail to give PNPCoH, but H<sub>2</sub> gives instead PNPCo(H)<sub>2</sub>, a result rationalized thermodynamically based on DFT calculations. Multiple equiv of PhSiH<sub>3</sub> give a product of Co(V), where N/SiPh and P/Si bonds have formed. N<sub>2</sub>CH(SiMe<sub>3</sub>) gives a 1:1 adduct of PNPCo, whose metric parameters suggest partial oxidation above Co<sup>I</sup>; N<sub>2</sub>CHPh gives a 1:1 adduct but with very different spectroscopic features. PhN<sub>3</sub> reacts fast, via several intermediates detected below 0 °C, to finally release N<sub>2</sub> and form a Co<sup>I</sup> product where one phosphorus has been oxidized, PN(P=NPh)Co. Whereas PNPCo(N<sub>3</sub>) resists loss of N<sub>2</sub> on heating, one electron oxidation gives a rapid loss of N<sub>2</sub>, and the remaining nitride nitrogen is quickly incorporated into the chelate ligand, giving [tBu<sub>2</sub>PCH<sub>2</sub>SiMe<sub>2</sub>NSiMe<sub>2</sub>NP(tBu<sub>2</sub>)=CH<sub>2</sub>Co]. O<sub>2</sub> or PhI=O generally gives products where one or both phosphorus centers are converted to its oxide, bonded to cobalt.

## Introduction

We have reported<sup>1</sup> the synthesis and characterization of (PNP)Co, where PNP is the monoanion (tBu<sub>2</sub>PCH<sub>2</sub>SiMe<sub>2</sub>)<sub>2</sub>N<sup>−</sup>, as a three-coordinate T-shaped species devoid of agostic interactions. The somewhat-low oxidation state of this metal qualifies it as a potential reducing agent but it is unclear whether the final oxidation state will be +2 or +3. Moreover, because d<sup>8</sup> (PNP)Co has a spin triplet ground state, all of its redox reactivity involves a change of spin state.<sup>2–5</sup> An earlier report<sup>1</sup> on the reaction of (PNP)Co with traditional Lewis bases, L, showed some evidence for diminished adduct formation enthalpies, which can originate from the spin pairing energy penalty in forming singlet (PNP)CoL. We now report on the reactivity of (PNP)Co toward potential one- and two-electron oxidants, including some unconventional ones: O<sub>2</sub>, PhN<sub>3</sub>, N<sub>3</sub><sup>−</sup>, RSiH<sub>3</sub>, I<sub>2</sub>, and RR'CN<sub>2</sub>. These latter are potential precursors to M=CR<sub>2</sub>, M=NR, M=O, M≡CR, and M≡N ligands. These results more fully define how the reducing power of (PNP)Co, already established to be greater than its rhodium analog by CO stretching frequencies, is not limited to occur exclusively at the metal center. Some of these results have been communicated previously.<sup>6,7</sup>

## Results and Discussion

The pincer ligand chosen in this work, (tBu<sub>2</sub>PCH<sub>2</sub>SiMe<sub>2</sub>)<sub>2</sub>N<sup>−</sup>, is a sufficiently potent donor that three-coordinate (PNP)Co, **1**,

even if it is far short of an 18 valence electron count, still has the potential to act as a reducing agent. Here, we probe the limits of this expectation and show it to be true but with certain subtle variations.

**Reaction with One-Electron Oxidants.** We first looked at the propensity of **1** to react with radical one-electron donors and reagents that are sources of A<sup>•</sup> (A = halogen or hydrogen). The reaction of equimolar quantities of **1** and the free radical galvinoxyl resulted in a rapid color change from green to red. The <sup>1</sup>H NMR spectrum now exhibited eight paramagnetically shifted resonances, consistent with the addition of galvinoxyl to form a single new product. Mass spectroscopy confirmed this to be PNPCoGalvinoxyl, **2**. The solution magnetic moment (3.96μ<sub>B</sub>) supports a formal oxidation of the cobalt center to a high-spin (distorted-tetrahedral) Co(II) and the concomitant formation of an aryloxy anionic ligand. Crystallization by cooling a saturated pentane solution and subsequent analysis by X-ray diffraction further confirmed the formation of **2** (Figure 1) formed by a rapid radical combination reaction between **1** and galvinoxyl.

The structure around Co<sup>II</sup> is indeed distorted tetrahedral, though there are significant distortions compared<sup>1</sup> to the solid-state structures of PNPCoI, PNPCo(OTf), and even when compared to PNPCo(anilide),<sup>1</sup> due to change in ortho substituents from methyls in PNPCo(anilide), to significantly larger tBu groups in **2**. These effects include, (1) a significant elongation of the P–Co bond lengths in **2** (P1–Co = 2.5732(7) Å, P2–Co = 2.5851(7) Å, average in PNPCoI = 2.44 Å, in anilide, 2.51 Å and in PNPCo(OTf), = 2.41 Å); (2) an opening of the N–Co–X angle (in **2** N1–Co–O1 = 128.39(7)°,

(1) Ingleson, M. J.; Pink, M.; Fan, H.; Caulton, K. G. *Inorg. Chem.* **2007**, *46*, 10321.(2) Poli, R. *J. Organomet. Chem.* **2004**, *689*, 4291.(3) Cacelli, I.; Poli, R.; Quadrelli, E. A.; Rizzo, A.; Smith, K. M. *Inorg. Chem.* **2000**, *39*, 517.(4) Poli, R. *Acc. Chem. Res.* **1997**, *30*, 494.(5) Poli, R. *Chem. Rev.* **1996**, *96*, 2135.(6) Ingleson, M. J.; Pink, M.; Caulton, K. G. *J. Am. Chem. Soc.* **2006**, *128*, 4248.(7) Ingleson, M.; Fan, H.; Pink, M.; Tomaszewski, J.; Caulton, K. G. *J. Am. Chem. Soc.* **2006**, *128*, 1804.

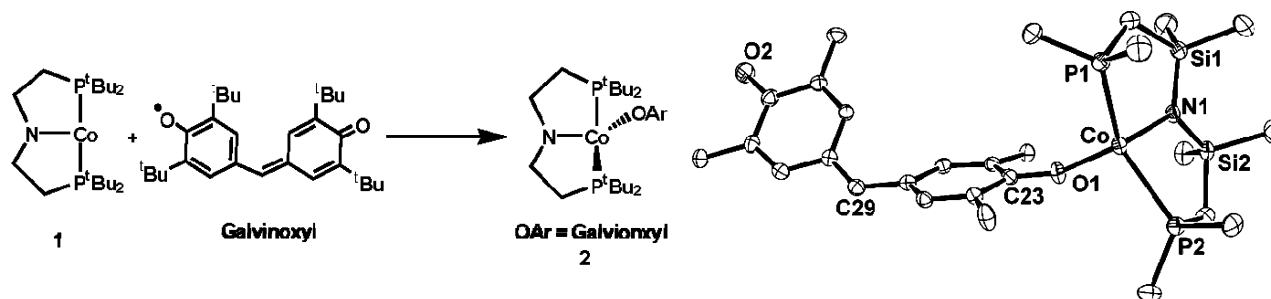


**Figure 1.** Left, The oxidation of cobalt in **1** by reaction with the free radical galvinoxyl. Right, ORTEP view (50% probabilities) of **2** (<sup>*t*</sup>Bu carbons and hydrogens omitted for clarity). Selected bond lengths (Å) and angles (°): Co–N1, 1.9663(18); Co–P1, 2.5732(7); Co–P2, 2.5851(7); Co–O1, 1.8936(15); P1–Co–P2, 137.44(2); N1–Co–O1, 128.39(7); P1–Co–O1, 109.46(5); P2–Co–O1, 102.22(5); P1–Co–N1, 92.70(6); P2–Co–N1, 89.14(6).

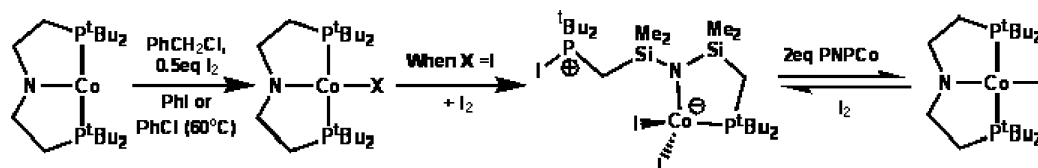


**Figure 2.** Reactivity of PNPCo and PNPCoX with halides/benzyl halides and phenyl halides.

whereas in PNPCoI, 117.45(4)° and in PNPCo(anilide), 118.95(11)°; (3) a compression of the N1–Co–P angles (in **2** 92.70(6)° and 89.14(6)° compared to an average in PNPCoI of 93.51°, in anilide 90.4° and in PNPCo(OTf) of 95.69°). All of these structural changes are required to accommodate the ortho <sup>*t*</sup>Bu groups of galvinoxyl, thereby allowing for the close approach of oxygen to cobalt. The galvinoxyl phenoxy containing O1 is twisted to be orthogonal to the P–Co–P plane, thereby minimizing steric repulsion with PNP. The Co–O1 distance (1.8936(15) Å) in **2** is fully consistent with other high-spin four-coordinate Co(II) aryloxy complexes;<sup>8</sup> however on comparison, the severe steric encumbrance in **2** does manifest itself further by inducing a considerable opening of the Co–O1–C23 angle (158.16(15)°). There is a significant twisting around C29, preventing any conjugation between aryl rings and precluding any further ligand reduction (e.g., oxidation to Co<sup>III</sup> would result in a ligand-based radical that could be delocalized through both aryl rings).

Following the ease of oxidation of **1** with the free radical galvinoxyl, we next probed the reactivity of **1** with respect to potential X atom donors (X = Cl or I). Reaction of **1** with PhCH<sub>2</sub>Cl rapidly forms PNPCoCl and half of an equiv of PhCH<sub>2</sub>CH<sub>2</sub>Ph. There is no further reaction between PNPCoCl and excess PhCH<sub>2</sub>Cl. **1** also readily reacts with iodobenzene at 25 °C, generating PNPCoI quantitatively. The more-challenging chlorobenzene required heating to 60 °C to activate the C–Cl bond (at 25 °C **1** is recovered unchanged after 18 h in the presence of 5 equiv of PhCl), producing PNPCoCl quantitatively (by <sup>1</sup>H NMR). **1** also reacts with 0.5 equiv of I<sub>2</sub>, predominantly forming PNPCoI.<sup>1</sup> However, small quantities of [κ<sup>2</sup>-(<sup>*t*</sup>Bu<sub>2</sub>P(I)CH<sub>2</sub>SiMe<sub>2</sub>NSiMe<sub>2</sub>CH<sub>2</sub>P(<sup>*t*</sup>Bu)<sub>2</sub>)CoI<sub>2</sub> and **1** are also present due to the secondary reaction that occurs between PNPCoI and I<sub>2</sub>. The reverse reaction, [κ<sup>2</sup>-(<sup>*t*</sup>Bu<sub>2</sub>P(I)CH<sub>2</sub>SiMe<sub>2</sub>NSiMe<sub>2</sub>CH<sub>2</sub>P(<sup>*t*</sup>Bu)<sub>2</sub>)CoI<sub>2</sub> returning to complex PNPCoI, is enabled by the addition of 2 equiv of **1**. This redox reaction simply involves two molecules of **1** undergoing one-electron oxidations at cobalt while a single phosphonium cation in [κ<sup>2</sup>-(<sup>*t*</sup>Bu<sub>2</sub>P(I)CH<sub>2</sub>SiMe<sub>2</sub>NSiMe<sub>2</sub>CH<sub>2</sub>P(<sup>*t*</sup>Bu)<sub>2</sub>)CoI<sub>2</sub> is reduced by two electrons. These results are summarized in Figure 2.

Following the successful oxidation of **1** with halogen atom donors, we targeted the synthesis of PNPCoH by the reaction of **1** with molecules with weak X–H bonds as potential hydrogen-atom donors. Radical metal complexes are well documented to abstract a hydrogen atom from silanes, stannanes, and even homolytically split H<sub>2</sub> (e.g., the reaction of TpCoN<sub>2</sub> with 0.5 equiv of H<sub>2</sub> yields<sup>9</sup> TpCoH). However, there is no reaction of **1** with <sup>*n*</sup>Bu<sub>3</sub>Sn–H (BDE Sn–H = 74 kcal·mol<sup>–1</sup>). To eliminate the possibility that the steric encapsulation that enshrouds the cobalt center in **1** may be preventing any reaction from taking place, the smaller H• atom source 1,4 cyclohexadiene (BDE C–H = 77 kcal·mol<sup>–1</sup>) was reacted with **1**, again without success (18 h at 25 °C). Therefore, steric bulk is not the insurmountable factor; instead it is reasonable that the failure stems from the Co–H bond in the hypothetical PNPCoH being weaker than the X–H bonds of these reagents (entirely consistent with the proposed<sup>1</sup> weak Co–R bond to be the origin<sup>6</sup> of reductive alkylation of **1** rather than simple metathesis). Thus, **1** can be readily oxidized by one-electron, provided the resultant Co–X bond is sufficiently strong to provide a driving force (the BDE Sn–H in <sup>*n*</sup>Bu<sub>3</sub>SnH at 74 kcal·mol<sup>–1</sup> is comparable to that of C–Cl for benzyl chloride, 72 kcal·mol<sup>–1</sup>). Therefore, as we have previously discussed,<sup>6</sup> the reducing power of PNPCo is strongly dependent on not only the redox potential of cobalt but also, equally importantly, on the energy recouped in the formation of new Co–X bonds.

**Oxidative Addition Reactions of H–H and Si–H.** We investigated the simple reaction of **1** with H<sub>2</sub>, envisaging a number of possible outcomes involving oxidative addition or heterolytic activation of dihydrogen. Any homolytic cleavage of H<sub>2</sub> might be discounted due to the high H–H bond dissociation energy (104.2 kcal·mol<sup>–1</sup>); furthermore a simple σ complex from an intact H<sub>2</sub> moiety was doubtful due to weak donors displaying no propensity to bond to cobalt in **1** because of the spin pairing penalty discussed earlier.<sup>1</sup> Exposure of a

(8) Jenkins, D. M.; Peters, J. C. *J. Am. Chem. Soc.* **2005**, *127*, 7148.

(9) Jewson, J. D.; Liable-Sands, L. M.; Yap, G. P. A.; Rheingold, A. L.; Theopold, K. H. *Organometallics* **1999**, *18*, 300.

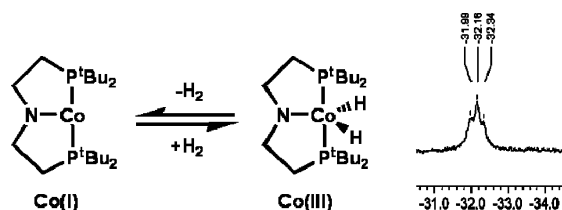


**Figure 3.** Reversible addition of  $\text{H}_2$  to cobalt in **1**. Right, the hydride region of the  $^1\text{H}$  NMR spectrum of  $\text{PNPCo}(\text{H})_2$  (298 K,  $\text{C}_6\text{D}_6$ ) showing the broad triplet resonance for  $\text{Co}-\text{H}$ .

degassed  $\text{C}_6\text{D}_6$  solution of **1** to ca. 4 atm of  $\text{H}_2$  produced an immediate color change to yellow/brown. The subsequent  $^1\text{H}$  NMR spectrum at 25  $^\circ\text{C}$  revealed only a partial conversion of **1** to a single new diamagnetic product that displayed  $\text{C}_{2v}$  symmetry on the NMR time scale, a broad two-hydride resonance (this intensity is repeatable over a number of independently prepared samples) at high field (triplet,  $-32.2$  ppm,  $J_{\text{H-P}} = 51$  Hz Figure 3), and a very broad  $^{31}\text{P}\{^1\text{H}\}$  NMR resonance at 89.9 ppm. These findings are consistent with the formation of a  $\text{Co}(\text{III})$  dihydride complex,  $\text{PNPCo}(\text{H})_2$ , **3**, that is in dynamic equilibrium with **1**, illustrated by vacuum removal of  $\text{H}_2$ , yielding pure **1** (by  $^1\text{H}$  NMR). This process is fully reversible, recharging with  $\text{H}_2$ , reproducing the incomplete conversion to **3**. Cooling a solution of **1** under ca. 4 atm of  $\text{H}_2$  to 205 K results in nearly complete conversion to **3**. The  $^1\text{H}$  and  $^{31}\text{P}\{^1\text{H}\}$  NMR spectra at this temperature reveal no additional fine coupling, with the inherent broadness an intrinsic property of atoms directly bound to quadrupolar cobalt. This frustrated attempts at determining hydride number by collecting a  $^{31}\text{P}$  NMR spectrum with selective coupling to hydride, with no additional fine coupling observed. Attempts to observe any HD coupling constant by the addition of HD to **1** were also inconclusive, with **3** formed (by  $^{31}\text{P}\{^1\text{H}\}$  NMR) but the broad hydride resonance still only a triplet; the broad nature of this resonance (13 Hz fwhm) could easily conceal a small HD coupling that would be consistent with a stretched dihydrogen complex.

Extensive DFT(PBE) calculations were therefore performed on all possible products from the reaction between **1** and excess  $\text{H}_2$ . Figure 4 shows all of the calculated structures with singlet ground states and the respective electronic energies of their formation from **1** and  $\text{H}_2$ .

Complexes with an intact,  $\sigma$ -bound  $\text{H}_2$  ligand are not stationary states, with optimization of singlet  $\text{PNPCo}(\text{H}_2)$  converging to **3**, whereas triplet  $\text{PNPCo}(\text{H}_2)$  dissociates  $\text{H}_2$  during the geometry optimization, generating **1** and  $\text{H}_2$ . Inspection of the relative electronic energies shows (after the entropic factors of the addition of one/two molecules of  $\text{H}_2$  are considered) that there are only two feasible products, **3** and **B**. Hypothetical **B** can be ruled out due to the failure to observe an N-H resonance in the  $^1\text{H}$  NMR spectrum and the observation of only one hydride environment even at 205 K. The calculations therefore support our product assignment as the classical dihydride **3** and are moreover consistent with the observed near-thermoneutral conversion of **1** to **3**. The calculated structural metrics of **3** revealed a H7-H8 distance (1.63  $\text{\AA}$ ) that indicates H/H bond scission and a formal cobalt +3 oxidation state. The geometry around cobalt approximates to a trigonal bipyramid (or Y-shaped), with the major distortion the compression of the H7-Co-H8 angle (67.9 $^\circ$ ).

Dihydride **3** is formally electronically and coordinatively unsaturated but exhibits no inclination to bind in a low steric profile to two electron donors (e.g.,  $\text{PhCN}$ ). There are two complementary factors that may be inhibiting additional ligand binding,  $\pi$  donation by the amide nitrogen (acting as a 3e donor), and the strong trans effect of hydride that in any potential product would be located trans to the incoming ligand.

In spite of this, **1** and **3** can be envisaged as two key resting states on a catalytic alkene hydrogenation cycle (Figure 5); therefore their utility as homogeneous hydrogenation catalysts was investigated.<sup>10</sup> An initial test reaction was promising, with rapid hydrogenation of ethene occurring at room temperature in  $\text{C}_6\text{D}_6$ , a rare occurrence for cobalt complexes.  $^1\text{H}$  NMR studies on this reaction mixture revealed the expected equilibrium mix of **1/3**. Unfortunately, attempts to hydrogenate the substituted alkenes, 1-hexene, and cyclohexene (50 equiv) with **1** under ca. 4 atm of  $\text{H}_2$  failed at room temperature. This is attributable to the severe steric encapsulation of the cobalt center disfavoring the alkene approach, with the **1/3** mix formed in an identical manner to that observed in the successful hydrogenation of ethene (by  $^1\text{H}$  NMR). Heating to 60  $^\circ\text{C}$  did initiate limited hydrogenation (1-hexene TOF = 1.05 mol/h, cyclohexene TOF = 0.70 mol/h); the slower rate observed for the disubstituted alkene further substantiates steric blocking as the retarding factor in the catalysis. It is noteworthy that, during the hydrogenation of 1-hexene, isomerization to internal alkenes was also observed, implying that the rates of reductive elimination and  $\beta$  hydride elimination from putative  $\text{PNPCo}(\text{H})(\text{R})$  are comparable.

We next attempted to determine if **1** could oxidatively add a Si-H bond and provide an analog to **3**, namely  $\text{PNPCo}(\text{SiR}_3)\text{H}$ . **1** is rapidly consumed by 4 equiv of  $\text{PhSiH}_3$ , forming a single, low-symmetry, pale-yellow, diamagnetic product; 1 equiv of  $\text{H}_2$  and  $\text{Ph}_2\text{SiH}_2$  were observed as byproducts (by  $^1\text{H}$  and  $^{29}\text{Si}$  NMR). Identification was only forthcoming when crystals suitable for X-ray diffraction analysis were obtained from the slow evaporation of a 1:1 (% v/v) pentane/ $\text{Me}_4\text{Si}$  solution. This revealed the addition of 3 equiv of  $\text{PhSiH}_3$  to the cobalt center of **1**, yielding  $\{\kappa^2\text{-}^i\text{Bu}_2\text{PCH}_2\text{Me}_2\text{SiNSiMe}_2\text{CH}_2^i\text{Bu}_2\text{P}(\text{H})\text{Si}=\}\text{Co}(\text{H})_3(\text{SiH}_2\text{Ph})_2$ , **4** (Figures 6 and 7). The structure consists of a formally  $\text{Co}(\text{V})$  center ligated by three hydrides (freely refined from the penultimate Fourier difference map), two primary silanes, a phosphine, and a base-( $\text{R}_3\text{P}$ )-stabilized silylene formed by cleaving one Si-C bond and two Si-H bonds of one silicon. The Co-Si bond distance of the silylene (2.1848(8)  $\text{\AA}$ ) is shorter than the two pure  $\sigma$  bonded Co-Si( $\text{Ph}$ ) $\text{H}_2$  groups (2.2622(9) and 2.2477(8)  $\text{\AA}$ ), confirming some multiple bond character in the Co-Si3 bond. The pure  $\sigma$  Co-Si bonds are comparable to the only other  $\text{Co}(\text{V})$ -silane complex structurally characterized,<sup>11</sup>  $\text{Cp}^*\text{Co}(\text{H})_2(\text{SiHPh}_2)_2$ , (Co-Si = 2.2492(21) and 2.2536(19)  $\text{\AA}$ ) and as expected (due to the reduced ionic radius of cobalt in the +5 oxidation state) are slightly shorter than  $\text{Co}(\text{III})$ -Si bonds (2.28–2.30  $\text{\AA}$ ).<sup>11</sup> The Si3-P2 bond length is fully consistent with other phosphine stabilized silylenes,<sup>12,13</sup> confirming that it is a dative bond. The Si4-Si5 distance of

(10) Knijnenburg, Q.; Horton, A. D.; van der Heijden, H.; Kooistra, T. M.; Hettterscheid, D. G. H.; Smits, J. M. M.; de Bruin, B.; Budzelaar, P. H. M.; Gal, A. W. *J. Mol. Catal.* **2005**, 232, 151.

(11) Brookhart, M.; Grant, B. E.; Lenges, C. P.; Prosenc, M. H.; White, P. S. *Angew. Chem., Int. Ed.* **2000**, 39, 1676.

(12) Gusev, D. G.; Fontaine, F.-G.; Lough, A. J.; Zargarian, D. *Angew. Chem., Int. Ed.* **2003**, 42, 216.

(13) Kawamura, K.; Nakazawa, H.; Miyoshi, K. *Organometallics* **1999**, 18, 1517.



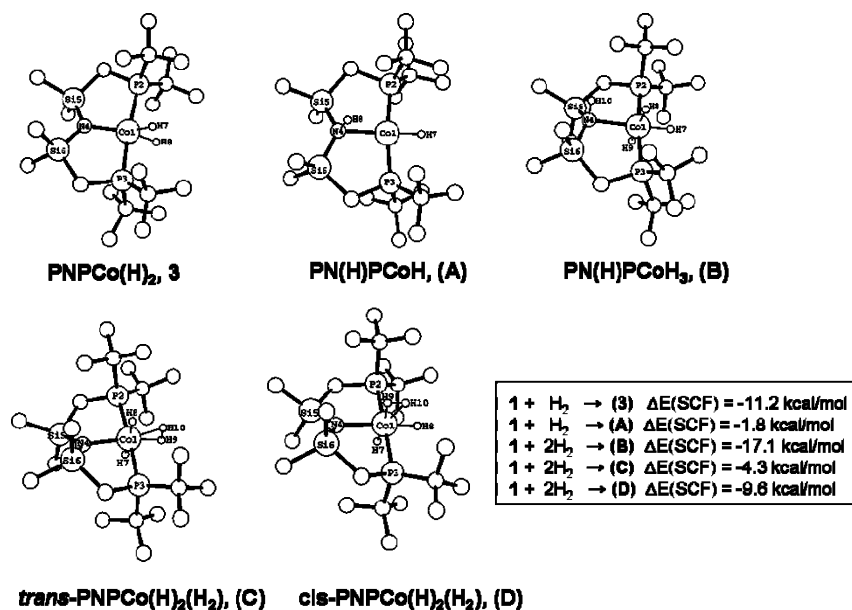


**Figure 4.** DFT geometry optimized structures for all of the possible complexes with a singlet ground state from the reaction between PNPCo and excess H<sub>2</sub>. Inset, the respective electronic energies for each conversion from 1.

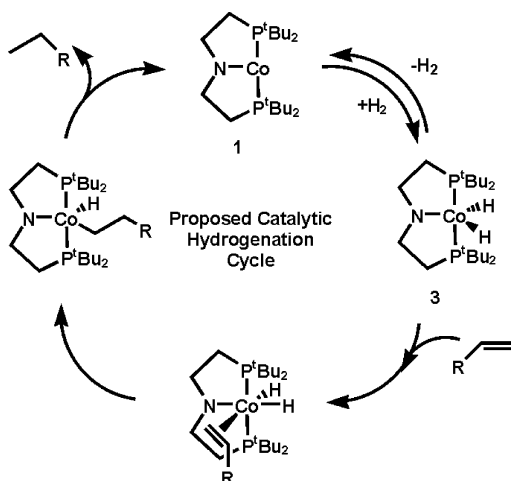


**Figure 5.** Proposed catalytic hydrogenation cycle commencing from 1.

3.726 Å is definitively nonbonding, confirming two PhH<sub>2</sub>Si<sup>−</sup> ligands, in contrast to a recent ambiguous case<sup>14,15</sup> where close Si–Si distances imply a lower oxidation state at the metal. The three inter-hydride distances are all greater than 2.0 Å, supporting a classical hydride structure. A closely related polyhydrido-based stabilized silylene osmium complex involving a PCP pincer ligand has also been recently reported<sup>12</sup> and also forms by the facile activation of numerous Si–H and Si–C bonds.

The NMR spectra for **4** are fully consistent with this formulation. The <sup>29</sup>Si NMR spectrum (Figure 8) displays five resonances of the expected multiplicity for <sup>1</sup>J coupling to protons (two triplets for inequivalent PhSiH<sub>2</sub>, one doublet for the base-stabilized silylene, and two singlets for ligand backbone SiMe<sub>2</sub>); the three multiplets all collapse to singlets on proton decoupling. The silylene chemical shift is at least ~50 ppm shifted downfield compared to the cobalt–silyl groups as expected. The <sup>31</sup>P{<sup>1</sup>H} NMR displays two resonances, one significantly broadened (concealing any fine coupling) due to direct bonding to

quadrupolar cobalt, and the second split into a doublet (<sup>3</sup>J<sub>P–P</sub> = 16 Hz) by coupling to phosphine. The <sup>1</sup>H NMR is complex, as expected for a low-symmetry molecule; the salient points are the observation of five Si–H resonances, consistent with diastereotopic Si–H on both Co–SiH<sub>2</sub>Ph groups. The fifth resonance, the silylene Si–H is split into a doublet (<sup>2</sup>J<sub>P–H</sub> = 50 Hz) due to coupling to phosphorus (collapses to a singlet in the <sup>1</sup>H{<sup>31</sup>P} NMR spectrum). A broad hydride resonance of intensity three with no observable fine coupling is present at −11.29 ppm. The high coordination number (7) leads to rapid fluxionality (the slow hydride exchange regime is not reached even at −70 °C), but the fluxionality is selective for hydride migration among inequivalent sites and does not involve site exchange between the two SiH<sub>2</sub>Ph ligands. Furthermore, there is no exchange between any Si–H and a hydride on cobalt.

Formulation of **4** as a Co(V) center based on X-ray diffraction data will always prove contentious, especially involving the possibility of classical/nonclassical hydrides. A number of experimental findings are relevant to the situation in **4**: (i) the observed lack of exchange between Co–H and free H<sub>2</sub> (or D<sub>2</sub>), (ii) no exchange between Si–H and Co–H (precluding a Co(III){η<sup>2</sup>-SiH<sub>2</sub>Ph}), (iii) the absence of H<sub>2</sub> evolution on extended evacuation, and (iv) no reaction (and specifically no H<sub>2</sub> evolution) between **4** and PhCN. All of these, combined with the existence<sup>11</sup> of a related Co(V) complex, ligated by silyl and hydride groups, support a Co(V) center in **4**.

The formation of **4** was unexpected, and the multistep reaction (Figure 7) occurs despite the mild conditions (25 °C). The reaction shows Si–C bond cleavage (ultimately forming Ph<sub>2</sub>-SiH<sub>2</sub>), multiple Si–H additions to cobalt, silylene formation, followed by phosphine migration from cobalt to silylene, and oxidation of d<sup>8</sup> Co(I) to d<sup>4</sup> Co(V). This complex reaction at 25 °C proceeds via an observable brown intermediate that can be characterized by repeating the reaction at −78 °C. The NMR spectra of this intermediate revealed a low-symmetry product, with silylene formation already evident by the characteristic <sup>31</sup>P{<sup>1</sup>H} NMR spectrum. Thus, the formation of the silylene moiety involving Si–C and multiple Si–H activation is extremely

(14) Chen, W.; Shimada, S.; Tanaka, M. *Science* **2002**, 295, 308.

(15) Crabtree, R. H. *Science* **2002**, 295, 288.

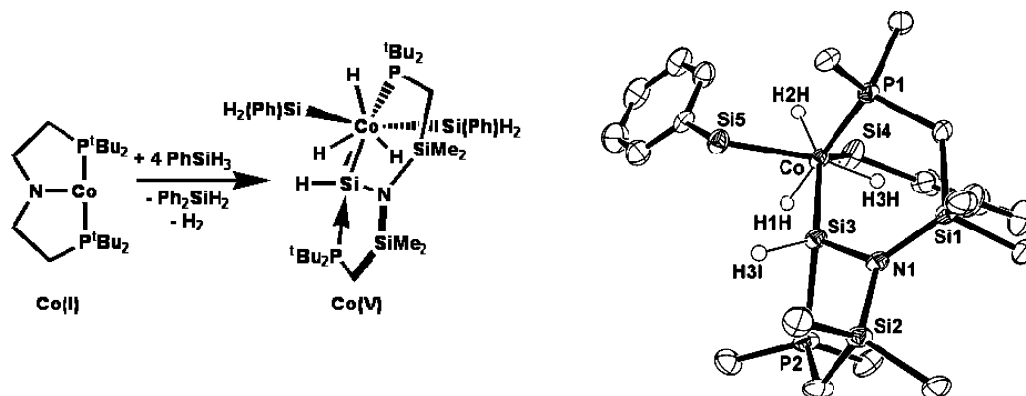


**Figure 6.** Left, the conversion of PNPCo to **4**, right ORTEP view (50% probabilities) of **4**. <sup>t</sup>Bu carbons and all hydrogens aside from Co–H and silylene Si–H are omitted for clarity. Selected bond lengths (Å) and angles (°): Co–P1, 2.267(8); Co–Si3, 2.1848(8); Co–Si4, 2.2622(9); Co–Si5, 2.2477(8); P2–Si3, 2.3783(10), N1–Si3, 1.774(2); Co–Si3–N1, 124.83(8); Co–Si3–P2, 122.94(4); P2–Si3–N1, 92.68(7).

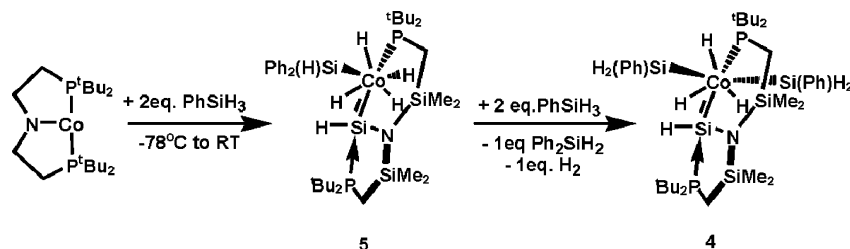


**Figure 7.** Reaction scheme displaying the reaction of PNPCo with 2 equiv of PhSiH<sub>3</sub> to generate intermediate **5** that upon addition of further PhSiH<sub>3</sub> leads to complete conversion to the structurally characterized **4**.

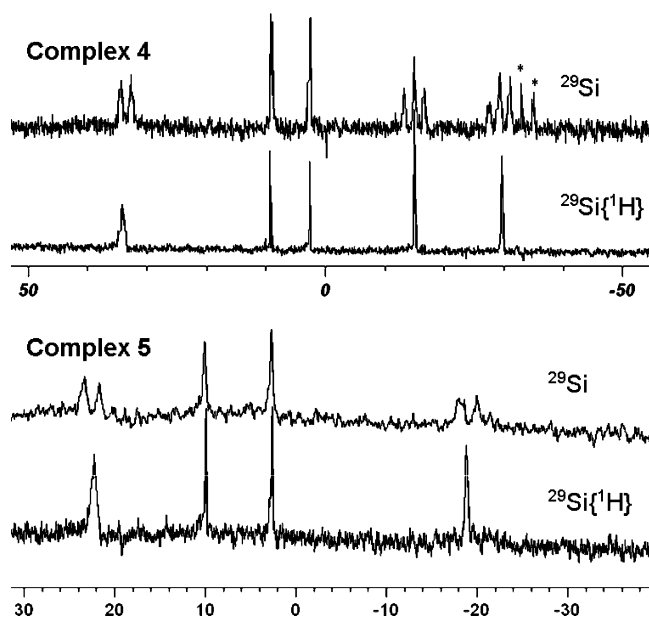


**Figure 8.** The <sup>29</sup>Si and <sup>29</sup>Si{<sup>1</sup>H} NMR spectra of, top, **4** (280 K, C<sub>6</sub>D<sub>6</sub>, \* = resonances due to Ph<sub>2</sub>SiH<sub>2</sub>), and bottom, **5** (263 K d<sub>8</sub>-toluene).

facile, occurring even at –78 °C. No simple oxidation product PNPCo(H)(SiPhH<sub>2</sub>) is observed at –78 °C.

An identical intermediate is observed in the addition of 1 equiv of PhSiH<sub>3</sub> to PNPCo at –78 °C, which on warming to 25 °C produces one new diamagnetic product (along with unreacted **1**). In the <sup>1</sup>H NMR, this product, **5**, displays an integral four-hydride resonance along with three signals in the Si–H region (consisting of one singlet and one doublet for the silylene proton, <sup>2</sup>J<sub>P–H</sub> = 49 Hz); the <sup>31</sup>P{<sup>1</sup>H} NMR is similar to that observed for **4**. The <sup>29</sup>Si NMR spectrum is especially informative (Figure 8), revealing four resonances, two doublets (one shifted

downfield corresponding to the silylene moiety), and two singlets (for the SiMe<sub>2</sub> ligand backbone); both doublets collapse to singlets on proton decoupling. A structure fully consistent with the spectroscopic data is a close analog of **4**. **5** is also a Co(V) complex and retains the Ph<sub>2</sub>HSi fragment that is prearranged to undergo reductive elimination of diphenylsilane. Similar facile Si–H/M–R redistributions are well documented.<sup>12</sup> Addition of further PhSiH<sub>3</sub> to **5** does indeed produce **4** along with 1 equiv of Ph<sub>2</sub>SiH<sub>2</sub> (and presumably H<sub>2</sub>). **5** can be cleanly synthesized by the addition (at –78 °C) of 2 equiv of PhSiH<sub>3</sub> to (PNP)Co. Both **4** and **5** are indefinitely stable in the solid state under argon but decompose completely in toluene solutions (at 25 °C) within 24 h to generate intractable mixtures. Taken together, these observations show an extremely low barrier to multiple silane activation and insertion into P–Co and N–Co bonds, whereas the observed formation of **4** and **5** implies that both contain an electrophilic silylene intermediate that is attacked by the nucleophilic phosphine, with the formation of the new Si–N bond providing the overall driving force for this conversion.

The purity observed in the complex transformation of **1** to **4** (which is quantitative by NMR) is explained by the lack of reactivity we independently observed between Ph<sub>2</sub>SiH<sub>2</sub> and **1**. Simply moving from a primary to a secondary silane switches off all reactivity, with the steric repulsion now sufficient to prevent the first step on this cascade reaction. **1** also failed to react with Et<sub>3</sub>SiH.

The higher oxidation states observed for cobalt in **4**, **5**, and PNPCo(H)<sub>2</sub> combined with the inability to exceed the Co(II) oxidation state with conventional oxidants reveal that hydride and silyl ligands are integral to reaching PNPCo(III). This may in part arise because these ligands allow for the formation of new bonds to cobalt without significantly reducing the electron

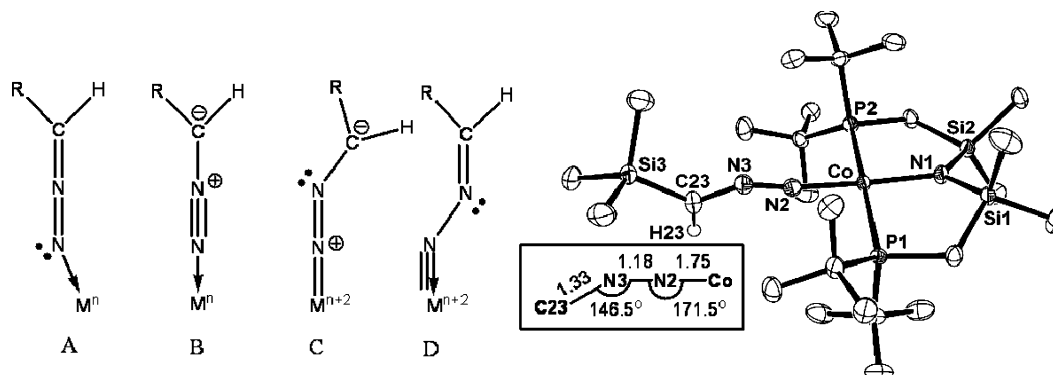


**Figure 9.** Left, possible terminal nitrogen  $\eta^1$  coordination modes, **A** and **B** as a neutral ligand and **C** and **D** as a doubly negative ligand. Right, ORTEP view (50% probabilities) of **6** (most hydrogens are omitted for clarity and disorder in the PNP ligand is not shown). Inset, key structural metrics of the diazo functionality. Selected bond lengths (Å) and angles ( $^\circ$ ): Co–N1, 1.9148(15); Co–N2, 1.7519(16); N2–N3, 1.183(2); N3–C23, 1.331(2); Co–P1, 2.262(1); Co–P2, 2.249(1); N1–Co–N2, 175.56(6); N1–Co–P1, 90.121(5); P1–Co–P2, 170.90(16); Co–N2–N3, 171.47(14), N2–N3–C23; 146.47(18); N3–C23–Si3, 120.53(15).

density (i.e., higher formal oxidation state) at the metal center due to their electropositive nature. Indeed, these ligands (and alkyls) are pervasive in metal complexes in high formal oxidation numbers (e.g., Cp\*ReH<sub>6</sub>, Cp\*IrH<sub>4</sub>, CpIrH<sub>2</sub>(SiR<sub>3</sub>)<sub>2</sub>)<sup>16–19</sup> due to their low electronegativity, resulting in metal ligand bonds with a significant covalent contribution thus rendering the oxidation-state formalism meaningless.

**Synthesis of Transient Electrophilic Co=E and Co≡E (E = CR<sub>2</sub>, NR, N, and O).** There has been significant recent progress in isolating stable mid-to-late 3d transition metal complexes with multiple bonds to simple ligands (e.g., M=O, M=S, M=NR, M≡N, M=CR<sub>2</sub>, M=PR).<sup>20–28</sup> Interest in molecules of this nature stems from their proposed involvement as key intermediates in a number of important catalytic atom/group transfer processes.<sup>29–33</sup> The ancillary ligand environment has proven to be the key to this success, with bulky, electron-rich ligands (two properties the PNP ligand certainly satisfies) a prerequisite for accessing these compounds. Furthermore, PNPCo has been shown to achieve the +3 oxidation state with certain reagents, so it is feasible that it would be able to support multiple bonds to these ligands. This applies particularly to carbenes, with their low-electronegativity carbon center and their close relationship to silylenes.

**a. N<sub>2</sub>CHR.**<sup>34–38</sup> Addition of a stoichiometric equiv of N<sub>2</sub>C(H)SiMe<sub>3</sub> to a toluene solution of **1** produced an immediate color change from green to dark yellow. No gas evolution was

discernible, suggesting an intact diazoalkane unit, a fact supported by the observation of an intense peak in the infrared spectrum at 2069 cm<sup>–1</sup> that corresponds to a coordinated cumulene. The <sup>1</sup>H NMR spectrum revealed the formation of a single new diamagnetic C<sub>2v</sub> symmetric product that displayed an unusual resonance for the unique methine C–H of the diazo functionality at –3.04 ppm. The dramatic upfield shift of this resonance can be attributed to significant carbanionic character at carbon (structures **B** or **C** in Figure 9). It is important to note that structures **B** and **C** differ by a change in the oxidation state at the metal, which emphasizes the ability of diazoalkanes to act as a  $\sigma$  donor and a  $\pi$  acid, even to the extent of accepting two electrons and forming a metal–imido complex. In this case, a significant contribution from structure **D** can be discounted because this produces diazoalkane methine C–H resonances in the range of 7 to 9 ppm. Unambiguous characterization of the diazoalkane binding mode was provided by an X-ray diffraction study (Figure 9) on crystals grown from (Me<sub>3</sub>Si)<sub>2</sub>O at –40  $^\circ$ C, which revealed the formation of PNPCo(N<sub>2</sub>C(H)–SiMe<sub>3</sub>), **6**, with the diazo moiety intact and bound in an  $\eta^1$  fashion through the terminal nitrogen.

The geometry around cobalt approximates to square planar, with unremarkable bond lengths and angles associated with the PNP ligand. More interestingly, the distances and angles associated with the diazo moiety do not conform to any of the Lewis structures shown in Figure 9, with a short Co–N2 bond (in comparison to Co–N1), short N–N and N–C bonds, an essentially linear N3–N2–Co angle, and an angle of 146.47–(18) $^\circ$  at N3. Inspection of the space-filling diagram for **6** reveals no close contacts between the diazo SiMe<sub>3</sub> and any of the four ligand <sup>t</sup>Bu groups; therefore, steric impact will have a minimal effect on the diazoalkane binding motif; thus electronic factors, specifically the degree of metal-to-ligand electron transfer is the dominant factor. Comparison of the Co–N2 bond length (1.7519(16) Å in **6**) with a related complex (PhB(CH<sub>2</sub>PPh<sub>2</sub>)<sub>3</sub>–Co–N<sub>2</sub>CPh<sub>2</sub>),<sup>39</sup> where full two-electron metal oxidation occurs

- (16) Herrmann, W. A.; Okuda, J. *Angew. Chem.* **1986**, 98, 1109.
- (17) Gilbert, T. M.; Bergman, R. G. *Organometallics* **1983**, 2, 1458.
- (18) Fernandez, M. J.; Maitlis, P. M. *Organometallics* **1983**, 2, 164.
- (19) Shortland, A. J.; Wilkinson, G. J. *Chem. Soc., Dalton Trans.* **1973**, 872.
- (20) Mindiola, D. J.; Hillhouse, G. L. *J. Am. Chem. Soc.* **2002**, 124, 9976.
- (21) Vivic, D. A.; Jones, W. D. *J. Am. Chem. Soc.* **1999**, 121, 4070.
- (22) Mindiola, D. J.; Hillhouse, G. L. *J. Am. Chem. Soc.* **2001**, 123, 4623.
- (23) Melnikvitz, R.; Mindiola, D. J.; Hillhouse, G. L. *J. Am. Chem. Soc.* **2002**, 124, 3846.
- (24) MacBeth, C. E.; Thomas, J. C.; Betley, T. A.; Peters, J. C. *Inorg. Chem.* **2004**, 43, 4645.
- (25) Eckert, N. A.; Vaddadi, S.; Stoian, S.; Lachicotte, R. J.; Cundari, T. R.; Holland, P. L. *Angew. Chem., Int. Ed.* **2006**, 45, 6868.
- (26) Gregory, E. A.; Lachicotte, R. J.; Holland, P. L. *Organometallics* **2005**, 24, 1803.
- (27) Badiel, Y. M.; Krishnaswamy, A.; Melzer, M. M.; Warren, T. H. *J. Am. Chem. Soc.* **2006**, 128, 15056.
- (28) Dai, X.; Warren, T. H. *J. Am. Chem. Soc.* **2004**, 126, 10085.
- (29) Hu, X.; Meyer, K. J. *Am. Chem. Soc.* **2004**, 126, 16322.
- (30) Zhao, P.; Hartwig, J. F. *J. Am. Chem. Soc.* **2005**, 127, 12066.
- (31) Thyagarajan, S.; Shay, D. T.; Incarvito, C. D.; Rheingold, A. L.; Theopold, K. H. *J. Am. Chem. Soc.* **2003**, 125, 4440.
- (32) Shay, D. T.; Yap, G. P. A.; Zakharov, L. N.; Rheingold, A. L.; Theopold, K. H. *Angew. Chem., Int. Ed.* **2005**, 44, 1508.
- (33) Waterman, R.; Hillhouse, G. L. *J. Am. Chem. Soc.* **2003**, 125, 13350.

- (34) Dartiguenave, M.; Joelle Menu, M.; Deydier, E.; Yves, D.; Siebald, H. *Coord. Chem. Rev.* **1998**, 178–180, 623.
- (35) Hillhouse, G. L.; Haymore, B. L. *J. Am. Chem. Soc.* **1982**, 104, 1537.
- (36) Polse, J. L.; Kaplan, A. W.; Andersen, R. A.; Bergman, R. G. *J. Am. Chem. Soc.* **1998**, 120, 6316.
- (37) Cohen, R.; Rybtchinski, B.; Gandelman, M.; Rozenberg, H.; Martin, J. M. L.; Milstein, D. *J. Am. Chem. Soc.* **2003**, 125, 6532.
- (38) Guillemot, G.; Solari, E.; Floriani, C.; Rizzoli, C. *Organometallics* **2001**, 20, 607.

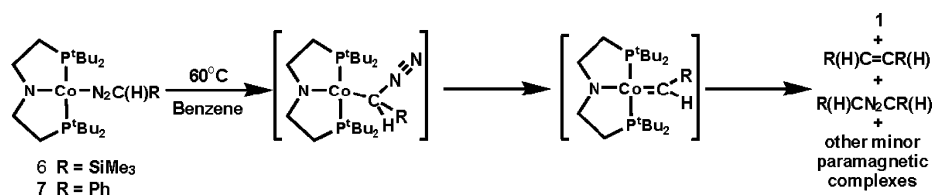


**Figure 10.** Decomposition of **6** and **7** on heating, with two proposed, but undetected, intermediates.

(Co–N = 1.667(2) Å), indicates an intermediate situation in **6** where there is metal-to-diazo electron transfer but short of full two-electron transfer, with its implied oxidation of cobalt to +3. The diazo group in **6** therefore lies somewhere on the continuum between Lewis structures **A** and **C**, with this intermediate diazo geometry a direct result of the reluctance of cobalt in PNPCo to undergo full oxidation to Co(III).

In an analogous reaction, the addition of 1 equiv of Ph(H)-CN<sub>2</sub> to **1** quantitatively (by <sup>1</sup>H NMR) led to a single new diamagnetic product, also possessing local C<sub>2v</sub> symmetry and a diazoalkane methine resonance shifted significantly upfield to –0.83 ppm. The lack of any gas evolution and the observation of a peak in the infrared spectrum corresponding to a coordinated cumulene led to the assignment of PNPCo(N<sub>2</sub>C(H)Ph), **7**. The only significant difference in the spectroscopic data between **6** and **7** (apart from those associated with the change in diazo R group) is a dramatic shift in the infrared vibration for the coordinated diazoalkane (from 2069 cm<sup>–1</sup> in **6** to 1592 cm<sup>–1</sup> in **7**). This must correlate to some degree of change in the bonding within the diazoalkane moiety in **7** because the infrared stretch of structurally characterized diazoalkane complexes only shifts by a maximum of ca. 100 cm<sup>–1</sup> on changing the diazoalkane substituents significantly (i.e., from N<sub>2</sub>CPh<sub>2</sub> to N<sub>2</sub>C(CO<sub>2</sub>Et)<sub>2</sub>, while maintaining the same metal complex and oxidation state). Despite repeated attempts, material suitable for single-crystal X-ray diffraction was not obtainable, frustrating definitive assignment of the bonding situation in the diazo fragment. The <sup>1</sup>H and <sup>13</sup>C{<sup>1</sup>H} NMR resonances for the diazo methine group (–0.83 and 41.5 ppm, respectively) eliminate structure **D** as a possibility; redox innocent binding (i.e., structure **A**) can also be discounted because a related complex,<sup>37</sup> (PCP)RhN<sub>2</sub>C(H)Ph (PCP = 1,3-C<sub>6</sub>H<sub>3</sub>-(CH<sub>2</sub>P<sup>i</sup>Pr)<sub>2</sub>), has a methine resonance in <sup>1</sup>H NMR at +3.76 ppm (close to free PhC(H)N<sub>2</sub> 4.8 ppm). Thus, a structure related to **C** but distinct from that observed in **6** is probable.

In solution, **6** and **7** are both stable at 25 °C for weeks; attempts to activate N<sub>2</sub> release by the addition of a Lewis acid catalyst (Sm(OTf)<sub>3</sub>)<sup>20</sup> resulted in no reaction after 48 h at 25 °C. Gentle heating (Figure 10, 60 °C in C<sub>6</sub>D<sub>6</sub>), however, results in the rapid consumption of the starting diazoalkane complex (no starting material remained after 4 h), with **1** being the major PNPCo-containing product detected (by <sup>1</sup>H NMR); other minor paramagnetic products are also present but have proven to be intractable. The products derived from the diazoalkane for both **6** and **7** are a mixture of the alkene and the azine products (by <sup>1</sup>H NMR); at no stage is a diamagnetic PNPCo(carbene) complex detected in either case. This is in distinct contrast to a related 4d congener (PCP)RhN<sub>2</sub>C(H)Ph that on warming evolves N<sub>2</sub> and cleanly forms a stable

rhodium–carbene complex.<sup>37</sup> The kinetic barrier observed in the reactivity of **6** and **7** is due to the requirement of a rearrangement from the nitrogen-bound to the carbon-bound diazoalkane isomer, which has been previously calculated to be the key intermediate for N<sub>2</sub> evolution and concomitant carbene formation. It is noteworthy that Peters' imido complex<sup>39</sup> PhB(CH<sub>2</sub>PPh<sub>2</sub>)<sub>3</sub>Co–N<sub>2</sub>CPh<sub>2</sub> is indefinitely stable, presumably due to a stronger Co–N bond preventing the required diazoalkane rearrangement, though steric inhibition of the C-bound isomer due to the presence of two phenyl groups may also contribute.

**b. RN<sub>3</sub>.** It is well documented that metal complexes that react with diazoalkanes to generate metal–imido species will in contrast react with organic azides to liberate N<sub>2</sub> and produce metal–nitrene complexes.<sup>38–46</sup> This distinct reactivity arises from a reduction in sterics and substitution of carbon by more-electronegative nitrogen, resulting in a greater negative charge at the key atom and thus a lower energy for the key intermediate. Targeting a metal–nitrene complex, PNPCo(III)NPh, a stoichiometric equiv of phenyl azide was added at –78 °C to **1** in pentane. Subsequent warming to room temperature led to gas evolution and to the formation of a dark-yellow solution, which on concentrating and cooling to –40 °C for 18 h yielded dark-yellow crystals in moderate yield. The <sup>1</sup>H NMR spectrum of these crystals revealed the formation of a new paramagnetic complex with local C<sub>s</sub> symmetry. Relevant precedents for ground-state triplets have been reported.<sup>47,48</sup> The solution magnetic moment (Evans Method) at 298 K of 3.40 μ<sub>B</sub> indicated a triplet, S = 1 cobalt center, consistent with either Co(I) or Co(III). The <sup>31</sup>P{<sup>1</sup>H} NMR spectrum displayed one broad, paramagnetically shifted resonance at 206.8 ppm, suggesting that at least one phosphine was no longer bound to the paramagnetic cobalt center. This was confirmed by an X-ray diffraction study, which revealed the formation of PN(P=NPh)-Co, **8** (Figure 11), a Co(I) complex with a P(V) phosphinimide functionality;<sup>49</sup> thus azide-to-nitrene transformation has occurred but the ultimate locus of oxidation by nitrene is at phosphorus, not cobalt.

The geometry around cobalt in **8** is still planar (angles sum to 360°), though the expansion of one of the five-membered

(39) Jenkins, D. M.; Betley, T. A.; Peters, J. C. *J. Am. Chem. Soc.* **2002**, *124*, 11238.

(40) Bart, S. C.; Lobkovsky, E.; Bill, E.; Chirik, P. J. *J. Am. Chem. Soc.* **2006**, *128*, 5302.  
 (41) Betley, T. A.; Peters, J. C. *J. Am. Chem. Soc.* **2004**, *126*, 6252.  
 (42) Matsunaga, P. T.; Hess, C. R.; Hillhouse, G. L. *J. Am. Chem. Soc.* **1994**, *116*, 3665.  
 (43) Proulx, G.; Bergman, R. G. *Organometallics* **1996**, *15*, 684.  
 (44) Brown, S. D.; Betley, T. A.; Peters, J. C. *J. Am. Chem. Soc.* **2003**, *125*, 322.  
 (45) Dai, X.; Kapoor, P.; Warren, T. H. *J. Am. Chem. Soc.* **2004**, *126*, 4798.  
 (46) Kogut, E.; Wiencko, H. L.; Zhang, L.; Cordeau, D. E.; Warren, T. H. *J. Am. Chem. Soc.* **2005**, *127*, 11248.  
 (47) Bart, S. C.; Chlopek, K.; Bill, E.; Bouwkamp, M. W.; Lobkovsky, E.; Neese, F.; Wieghardt, K.; Chirik, P. J. *J. Am. Chem. Soc.* **2006**, *128*, 13901.  
 (48) Rohde, J.-U.; Stubna, A.; Bominaar, E. L.; Muenck, E.; Nam, W.; Que, L., Jr. *Inorg. Chem.* **2006**, *45*, 6435.  
 (49) Dehnicke, K.; Strähle, J. *Polyhedron* **1989**, *8*, 707.



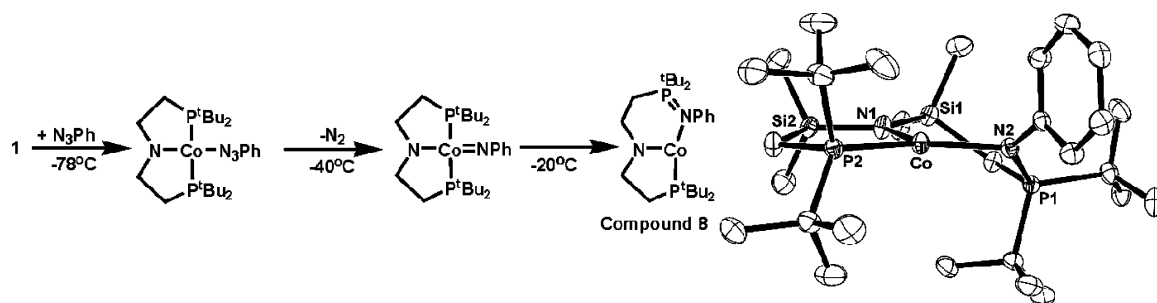


**Figure 11.** Left, proposed mechanism for the formation of **8**. Right, ORTEP view (50% probabilities) of **8** (hydrogens omitted for clarity). Selected bond lengths (Å) and angles (°): Co–N1, 1.9763(18) Å; Co–P2, 2.1838(6); Co–N2, 1.9866(6); N2–P1, 1.6043(6); P2–Co–N2, 153.77(5); P2–Co–N1, 97.04(5); N2–Co–N1, 109.6(7).

rings to six-membered by nitrene insertion results in a distortion away from the T-shaped structure observed for **1**. The N1 and N2 bond lengths are similar, confirming both as single Co–N bonds, whereas the P1–N2 distance is consistent with a double bond. The P2–Co bond length (2.1838(6) Å) is contracted somewhat when compared to those in compound **1** (Co–P1, 2.2281(6); Co–P2, 2.2237(6) Å); this presumably arises due to the reduced steric crowding around cobalt allowing for a shorter P2–Co bond to compensate for the poorer electron donating ability of the phosphinimide ligand. Similar nitrene insertions into ancillary ligands have been reported, one example<sup>29</sup> of particular relevance involving a Co(III) imido complex with an electrophilic nitrene group that inserts into a cobalt–carbene bond. A related mechanism can be envisaged here where a nucleophilic phosphine attacks a transient cobalt–nitrene complex (Figure 11), generating the observed Co(I) phosphinimide complex. Support for this mechanism is forthcoming from a low-temperature NMR study. Combination of stoichiometric equivalents of **1** and PhN<sub>3</sub> at –78 °C in d<sub>8</sub>-toluene followed by warming to –60 °C resulted in a color change from green to brown, and the <sup>1</sup>H NMR spectrum revealed the formation of a single new diamagnetic product with C<sub>2v</sub> symmetry and a relatively sharp phosphine resonance at 54.0 ppm in the <sup>31</sup>P{<sup>1</sup>H} NMR spectrum. This phosphorus chemical shift is extremely close to that observed for the coordinated diazoalkane complexes (52.3 and 48.5 ppm) and combined with the solution C<sub>2v</sub> symmetry lead us to assign this as the intact phenyl azide complex PNPCo(N<sub>3</sub>Ph). Warming this solution to –40 °C results in a second color change from brown to deep green, and NMR spectroscopy reveals the complete transformation of this diamagnetic compound to a single new paramagnetic complex with three significantly broadened resonances in the <sup>1</sup>H NMR, implying local C<sub>2v</sub> symmetry; no phosphorus resonance is now detectable. Repeating this experiment outside the NMR probe allowed for the visual detection of gas evolution at this temperature, confirming N<sub>2</sub> loss. We tentatively assign this new paramagnetic complex as the Co(III) imido complex PNPCo(NPh), which on further warming to –20 °C results in the rapid conversion to **8** (the reaction is complete within 10 min at this temperature). The narrow temperature stability window of PNPCo(NPh) has frustrated isolation of material for an X-ray diffraction study and subsequent unambiguous characterization.

Density functional theory (PBE) calculations were performed (Figure 12) using the complete ligand set to investigate the structure and frontier orbitals of PNPCo(NPh). The ground state is calculated to be *S* = 1, triplet PNPCo(NPh), 9.7 kcal·mol<sup>–1</sup>

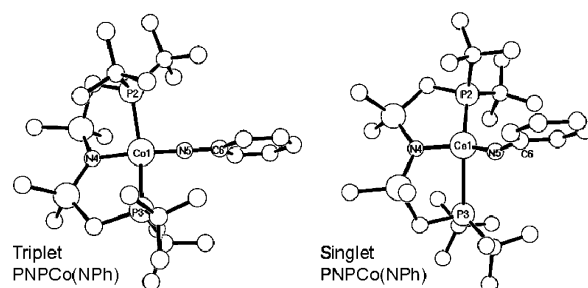


**Figure 12.** Left, DFT geometry optimized structure for triplet PNPCo(NPh), selected bond lengths (Å) and angles (°): Co1–P2, 2.384; Co1–P3, 2.397; Co1–N4, 1.855; Co1–N5, 1.830; P2–Co1–P3, 178.3; P2–Co1–N4, 89.9; N4–Co1–N5, 177.5; P2–Co1–N5, 89.4; C6–N5–Co1, 169.3. Right, DFT geometry optimized structure for singlet PNPCo(NPh), selected bond lengths (Å) and angles (°): Co1–P2, 2.65; Co1–P3, 3.002; Co1–N4, 1.879; Co1–N5, 1.666; P2–Co1–N4, 94.7; P2–Co1–N5, 109.6; N4–Co1–N5, 144.3; C6–N5–Co1, 153.8.

below the singlet isomer; this supports the assignment of the low-temperature paramagnetic intermediate observed as PNPCo(NPh). The ligand environment around cobalt in triplet PNPCo(NPh) is square planar (angles sum to 360°), a geometry with good precedent for four-coordinate triplet d<sup>6</sup> cobalt. The most noteworthy structural metric in triplet PNPCo(NPh) is the imido Co–N5 bond length (1.830 Å), which when compared to the cobalt–amide bond distance of 1.855 Å strongly suggests a bond order of close to 1. Cobalt imido complexes have the potential to have bond orders up to 3, involving one  $\sigma$  bond and two orthogonal  $\pi$  bonds. Structurally characterized, stable Co(III)-imido complexes consistently exhibit short Co–N bonds, indicative of significant multiple bond character, for example, 1.658(2) Å in PhB(CH<sub>2</sub>PPh<sub>2</sub>)<sub>3</sub>Co(N-*p*-tolyl)<sup>39</sup> and 1.624(4) Å in [ $\beta$ -diketiminato]CoN-Adamantyl,<sup>45</sup> whereas even in the thermally sensitive complex [TIMEN<sup>xyl</sup>]Co(N-*p*-OMe–C<sub>6</sub>H<sub>4</sub>)[BPh<sub>4</sub>] (TIMEN = tris-[2-(3-arylimidazol-2-ylidene)ethyl]amine, xyl = 2,6-dimethylphenyl)<sup>29</sup> the Co–N distance is 1.675(2) Å. It is no coincidence that these cobalt–imido complexes with their short Co=N distances are all low spin, *S* = 0, d<sup>6</sup> Co(III) complexes; spin pairing provides an additional empty d orbital that is available to participate in the stabilizing nitrogen-to-cobalt  $\pi$  donation. Triplet PNPCo(NPh), with an additional d orbital singly occupied (and therefore not available to participate in  $\pi$  bonding with the nitrene fragment) has a drastically elongated Co–N bond, which presumably contributes to its reactive nature. This requirement for sufficient empty d orbitals is exemplified by a second singlet stationary point (only 0.8 kcal·mol<sup>–1</sup> further above the most stable singlet isomer); this now has a calculated imido Co–N bond length of 1.666 Å. Thus, in mid-to-late



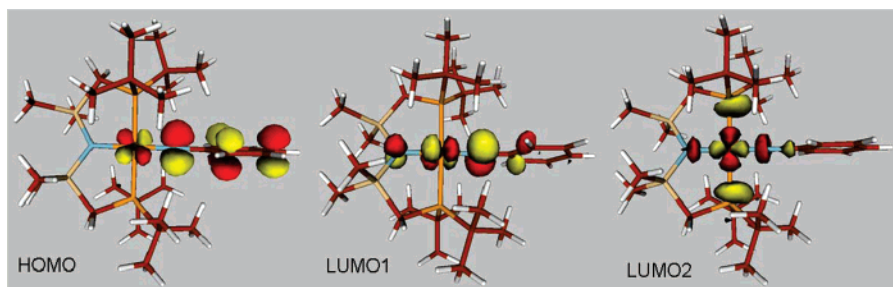


Figure 13. Calculated frontier molecular orbitals for singlet PNPCo(NPh).

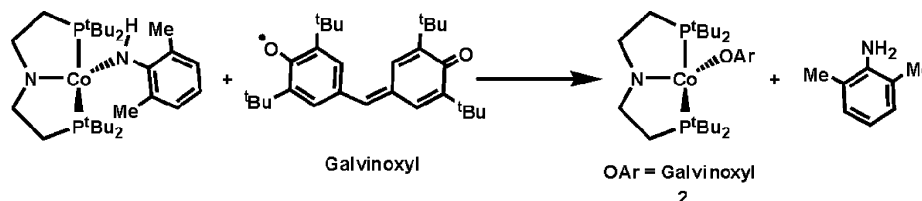


Figure 14. Reaction scheme for the combination of galvinoxyl radicals with (PNP)Co[NH(2,6-Me<sub>2</sub>-C<sub>6</sub>H<sub>3</sub>)].

transition metals low-spin ground states would appear to be a prerequisite for the formation of stable M=E bonds. The singlet state of PNPCo(NPh) is energetically close to the triplet and thus may be mechanistically relevant. Further examination of the structure and frontier orbitals reveals a number of key points: (1) the singlet PNPCo(NPh) (Figure 12) structure exhibits a dramatic lengthening (indicating complete Co/P dissociation) of one P–Co bond length (Co1–P3, 3.002 Å), resulting in a more nucleophilic phosphorus; (2) the LUMO for the singlet (Figure 13) reveals significant imide nitrogen character, therefore an electrophilic N(Ph). These two factors explain the origin of the observed low-energy barrier to P/N bond formation.

It is worth noting that similar findings have been previously reported by Peters et al.,<sup>24</sup> notably that, in the DFT optimized structure of [PhBP'Pr<sub>3</sub>]NiN'Bu, a d<sup>7</sup> S = 1/2 Ni(III) complex, there is one P–Ni distance significantly elongated. Of more relevance to this study is the calculated structure of a hypothetical d<sup>6</sup> Ni(IV) nitride complex, [PhBP'Pr<sub>3</sub>]Ni≡N, which optimizes with nitride inserted into a P–Ni bond. The major destabilizing effect in [PhBP'Pr<sub>3</sub>]Ni≡N arises from the presence of two unpaired electrons in high-energy orbitals (a triplet ground state is likely considering the small energy difference between the three high-energy orbitals), limiting  $\pi$  bonding between nitrido nitrogen and nickel.

A preliminary investigation into the reactivity of **8** reveals disparate behavior when compared to the related Co(I) **1**. Attempts to oxidize the Co(I) center of **8** with excess H<sub>2</sub> at 25 °C failed, with no reaction observed after 24 h; this confirms what is intuitively expected, that conversion of a 'Butyl phosphine ligand to a phosphinimide reduces the electron density at cobalt, thereby raising its oxidation potential. An attempt to react **8** with a second equiv of PhN<sub>3</sub> resulted in an intractable mixture, possibly due to the instability of Co(I) bound by two weaker electron donor phosphinimides. The reaction of a bulkier organic azide with **1** was attempted with the hope that unfavorable steric interactions would help prevent nitrene insertion into the P–Co bond; however, the addition of adamantyl azide to **1** resulted in no reaction (after 18 h at 25 °C, by <sup>1</sup>H NMR and IR).

**c. Other paths to an Arylimide.** With the cobalt–anilide complex (PNP)Co[NH(2,6-Me<sub>2</sub>-C<sub>6</sub>H<sub>3</sub>)] easily accessible,<sup>1</sup> we attempted to synthesize a PNPCo(imido) species via hydrogen-atom abstraction (stepwise, via electron, then proton transfer), a methodology that has been previously successful in generating nickel–imido complexes.<sup>20,33,50</sup> Reaction of (PNP)Co[NH(2,6-Me<sub>2</sub>-C<sub>6</sub>H<sub>3</sub>)] with the free radical TEMPO at 25 °C for 24 h and then at 60 °C for a further 24 h causes no reaction (by <sup>1</sup>H NMR). However, addition of 1 equiv of galvinoxyl radicals (O–H bond strength 70 kcal/mol<sup>51</sup>) to (PNP)Co[NH(2,6-Me<sub>2</sub>-C<sub>6</sub>H<sub>3</sub>)] in benzene at 25 °C resulted in the rapid and clean formation of **2** (Figure 14), PNPCo(galvinoxyl) (identified by its characteristic <sup>1</sup>H NMR); the galvinoxyl free radical has been reduced to an aryloxide but no concomitant oxidation of cobalt has occurred. Analysis of the nitrogen-containing products from this reaction revealed that the only amide derived species was 2,6-dimethyl aniline (by <sup>1</sup>H NMR comparison with commercial 2,6-dimethylaniline); no hydrazine or azo compounds were detectable. The exact one-to-one stoichiometry of the reaction is further confirmed by the absence of any hydrogen-atom abstraction product; namely, the alcohol of galvinoxyl or a radical coupled product galvinoxyl–N(H)(3,5-Me<sub>2</sub>-C<sub>6</sub>H<sub>3</sub>). The reaction proceeds identically in benzene or THF, and an attempt to identify any intermediates by a low-temperature NMR study in d<sub>8</sub>-toluene was uninformative with full conversion to **2** even at –70 °C, consistent with a rapid radical process.

The formation of 2,6-dimethyl aniline in this reaction suggests that the locus of oxidation is at the amide nitrogen, expelling an aminyl radical, Ar(H)N<sup>•</sup>, which then abstracts a hydrogen atom, presumably from the solvent. Without the observation of any intermediates and/or the identification of any solvent derived products, any further discussion is not warranted.

**d. A Terminal Nitride?** Following the success in accessing PNPCo=NR complexes (albeit with a limited temperature stability range), we next targeted a cobalt nitride complex of the general formula PNPCo<sup>X</sup>N; of particular interest was the case where X = +5 because this would then result in an

(50) Cowley, R. E.; Bontchev, R. P.; Sorrell, J.; Sarracino, O.; Feng, Y.; Wang, H.; Smith, J. M. *J. Am. Chem. Soc.* **2007**, *129*, 2424.

(51) Gupta, R.; Borovik, A. S. *J. Am. Chem. Soc.* **2003**, *125*, 13234.

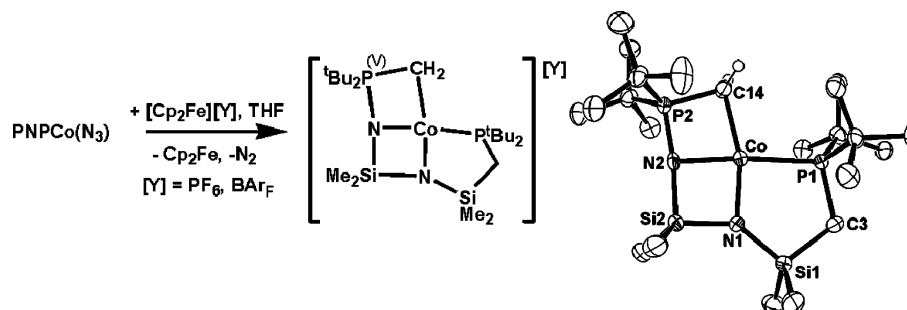


**Figure 15.** Left, schematic for the formation of **9** from the oxidation of  $\text{PNPCoN}_3$  by the ferrocenium cation. Right, ORTEP view (50% probabilities) of one of the two independent units (which are effectively identical) in the asymmetric unit. Selected bond lengths (Å) and angles (°): Co–N1, 1.856(4); Co–N2, 1.899(4); Co–C14, 2.041(6); Co–P1, 2.2927(16); P2–C14, 1.778(6); P2–N2, 1.613(5); Si2–N2, 1.720(5); Si2–N1, 1.714(5); Si1–N1, 1.718(4); Si1–C3, 1.892(6); N1–Si2–N2, 92.8(2); N2–P2–C14, 97.6(2); N2–Co–C14, 80.7(2); N2–Co–N1, 83.0(2); C14–Co–P1, 105.27(14) P2–N2–Si2, 62.8(3).

isoelectronic compound to the recently published<sup>52</sup> Ru(IV) complex,  $\text{PNPRuN}$ . Initial attempts to install a nitride functionality involved the reaction of  $(\text{PNP})\text{CoCl}$  with a stoichiometric equivalent of  $\text{Li}(\text{dbabh})$  ( $\text{dbabh} = 2,3:5,6\text{-dibenzo-7-aza bicyclo}[2.2.1]\text{hepta-2,5-diene}$ ) in THF (a reagent successfully used for this purpose by the Cummins and Peters groups).<sup>41,53</sup> However, even after long reaction times (48 h) there is no evidence for any amide formation, with only unreacted  $(\text{PNP})\text{-CoCl}$  present by  $^1\text{H}$  NMR; the lack of metathesis observed can be attributed to the steric bulk of the amide reagent.

As previously shown in the formation of  $\text{PNPRuN}$ , azide is a potential source of a nitride ligand, providing there is the required two-electron transfer:  $\text{N}_3^- + 2e \rightarrow \text{N}^{3-} + \text{N}_2$ .  $\text{PNPCoN}_3$  is recovered unchanged after 4 days refluxing in benzene, whereas Lewis acid catalysis of  $\text{N}_2$  release<sup>20</sup> utilizing  $\text{Sm}(\text{OTf})_3$  also revealed no reaction (18 h at 25 °C). Attempts to increase the reductive power of cobalt in  $\text{PNPCoN}_3$  by one-electron reduction with excess magnesium powder (or 1 equiv of sodium naphthalide) resulted in clean formation of **1** as the only  $\text{PNPCo}$  product with no  $\text{N}_2$  evolution; in this case azide is behaving like a *pseudo*-halide. Paradoxically, the oxidation of  $\text{PNPCoN}_3$  with the ferrocenium cation (as the  $\text{BARF}$  salt,  $\text{BARF} = [\text{B}(3,5\text{-C}_6\text{H}_3(\text{CF}_3)_2)_4]^-$ ) in THF at 25 °C resulted in rapid gas evolution and a subtle color change from terracotta to red. The  $^1\text{H}$  NMR ( $d_8\text{-THF}$ ) confirmed one-electron oxidation of  $\text{PNPCoN}_3$ , with  $\text{Cp}_2\text{Fe}$  present at 4.12 ppm, along with the formation of a single new paramagnetic complex of  $C_s$  symmetry. The mass spectrum (ESI+ mode) gave a molecular ion peak at 521.2  $m/z$  that corresponds to a compound with the empirical formula  $[\text{PNPCoN}]^+$ . Unambiguous characterization of this species was forthcoming from an X-ray diffraction study of crystals of the  $[\text{PF}_6]^-$  analog (which exhibits identical spectroscopic data for the cationic portion). This revealed that the compound is not the expected Co(V) nitride but a four-coordinate Co(III) complex (Figure 15) resulting from the formation of new P/N, C/Co, and N/Si bonds:  $[\text{Bu}_2\text{PCH}_2\text{Si}(\text{Me})_2\text{NSi}(\text{Me})_2\text{NP}(\text{Bu}_2)=\text{CH}_2\text{Co}]^+$ , **9**.

The crystal structure shows separated cations and  $\text{PF}_6^-$  ions together with a THF molecule filling void space but not involved in any significant interaction (i.e., to cobalt or via hydrogen bonding to  $\text{CH}_2\text{Co}$  hydrogens). The asymmetric unit contains two independent formula units with effectively identical geo-

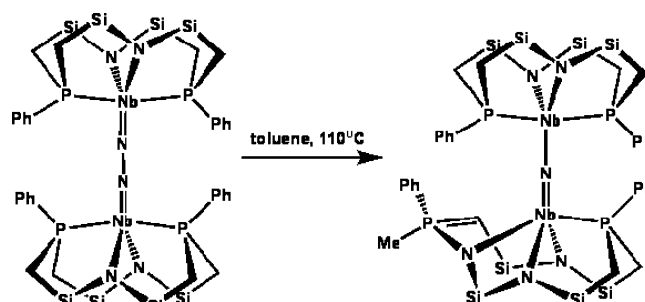


**Figure 16.** Conversion, on heating, of the dinitrogen-bridged niobium dimer to a nitride-bridged dimer with concomitant nitrogen inserted into the ligand backbone; silyl methyls omitted for clarity.

metrical parameters; therefore, we limit our discussion to one independent molecule. The structure reveals one azide-derived nitrogen atom (N2) inserted into the backbone of the ligand bonded to one phosphorus and one silicon. The environment around cobalt consists of two amides, one phosphine, and one carbon from a phosphorus ylide (both  $\text{CH}_2$  protons were located in the penultimate difference map) in a distorted square planar geometry (angles sum to 360.2°). The accompanying anion results in an oxidation state at cobalt of +3. Both nitrogens are strictly planar (angles sum to 359.9 and 359.7°) with the small difference in their respective bonds to cobalt (Co–N1, 1.856(4); Co–N2, 1.899(4)) attributable to the constraints imposed by the two fused four-membered rings. The three Si–N distances for **9** are identical within errors. The  $^1\text{H}$  NMR of **9** is consistent with this structure, displaying  $C_s$  symmetry with five paramagnetically shifted resonances (the  $2\text{H}$  intensity resonance of the ylide  $\text{CH}_2$  is not detectable because of its proximity to the paramagnetic cobalt center). The magnetic moment for **9** of  $3.0\mu_B$  at 298 K (Evans method,  $d_8\text{-THF}$ ) is consistent with a triplet ground state,  $S = 1$  Co(III)<sup>54</sup> center, which is a spin state with good precedent for four-coordinate, square planar cobalt.

The mechanism leading to **9** can be expected to be complex, requiring the breaking of Si–C and Co–N bonds while forming new C–Co, P–N, and Si–N bonds. There is literature precedent<sup>55</sup> for a related nitride insertion reaction, with Fryzuk's group, reporting that a dinitrogen-bridged niobium dimer on heating undergoes an insertion of nitrogen into the ligand backbone (Figure 16); a complex multistep mechanism via an

(52) Walstrom, A.; Pink, M.; Yang, X.; Tomaszewski, J.; Baik, M.-H.; Caulton, K. G. *J. Am. Chem. Soc.* **2005**, *127*, 5330.

(53) Mindiola, D. J.; Cummins, C. C. *Angew. Chem., Int. Ed.* **1998**, *37*, 945.

(54) Doerrer, L. H.; Bautista, M. T.; Lippard, S. J. *Inorg. Chem.* **1997**, *36*, 3578.

(55) Fryzuk, M. D.; Kozak, C. M.; Bowdridge, M. R.; Patrick, B. O.; Rettig, S. J. *J. Am. Chem. Soc.* **2002**, *124*, 8389.

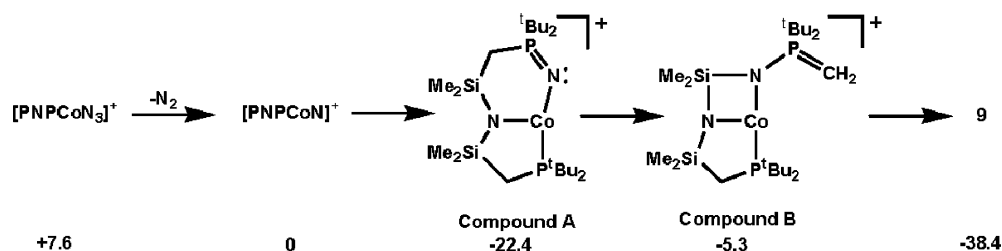


**Figure 17.** Proposed reaction scheme for the conversion of  $[\text{PNPCo}(\text{N}_3)]^+$  to **9**, with calculated electronic energies ( $\text{kcal}\cdot\text{mol}^{-1}$ ) of feasible intermediates.

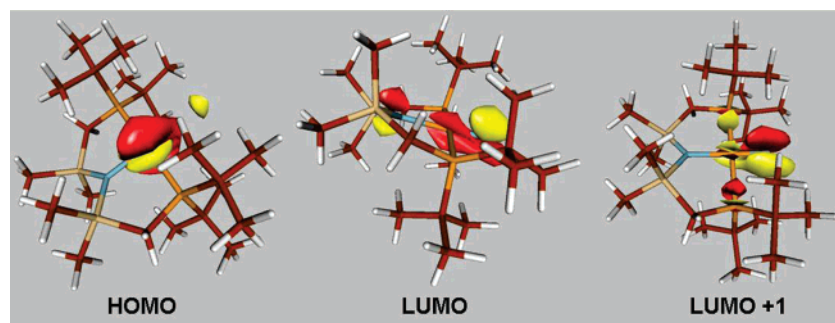


**Figure 18.** Frontier molecular orbitals calculated for singlet  $[\text{PNPCoN}]^+$ .

electrophilic niobium nitride complex and subsequent attack by nucleophilic phosphine is proposed.

In an effort to gain insight into the mechanism of the facile conversion of  $\text{PNPCoN}_3$  into **9**, a low-temperature NMR study in  $d_8$ -THF using  $\text{Cp}_2\text{Fe}[\text{BARF}]$  (for solubility reasons) was undertaken. Combining  $\text{PNPCoN}_3$  with  $[\text{Cp}_2\text{Fe}]\text{BARF}_4$  at  $-65^\circ\text{C}$  shows (by  $^1\text{H}$  NMR) complete consumption of the starting cobalt azide complex and the formation of  $\text{Cp}_2\text{Fe}$ , together with new broad peaks of a (low symmetry) paramagnetic product. At  $-50^\circ\text{C}$ , those peaks decline in intensity and while signals from two new paramagnetic compounds grow in, these begin to transform to the final crystallographic product (**9**) at  $-30^\circ\text{C}$ . At no temperature is any  $^{31}\text{P}\{^1\text{H}\}$  NMR resonance observed, indicating the absence of any detectable diamagnetic intermediates. In sum, the bond making and breaking reactions to form **9** involve at least three detectable intermediates, all paramagnetic in spite of all having an even number of electrons. A plausible reaction mechanism (Figure 17) can be proposed for the conversion of  $\text{PNPCoN}_3$  to **9** via at least three intermediates. Oxidation of  $\text{PNPCoN}_3$  by  $\text{Cp}_2\text{Fe}^+$  would yield  $[(\text{PNP})\text{Co}(\text{N}_3)]^+$  that can then evolve  $\text{N}_2$  and form a  $\text{Co}(\text{V})$  nitride  $[\text{PNPCoN}]^+$ . There is precedent, both in this work and from that of Peters and Meyers' groups,<sup>24,29</sup> for intramolecular attack by a nucleophilic ligand on a terminal nitrogen, which in this case would produce the  $\text{Co}(\text{III})$  complex  $[(\text{PNP}=\text{N})\text{Co}]^+$  (**A**). This P/N bond formation makes an initially electrophilic nitrogen more nucleophilic and thus able to attack silicon. Breaking the  $\text{Si}-\text{CH}_2$  bond then becomes possible because the  $\text{P}(\text{V})$  center can stabilize the emerging  $\text{CH}_2$  carbanion by ylide formation (**B**). As the  $\text{Si}/\text{C}$  bond cleaves, the developing electrophilic character at silicon can be stabilized by binding to electron-rich nitrogen on phosphorus (**B**). Closing the second four-membered ring by nucleophilic ylide carbon binding to  $\text{Co}$  (**B**  $\rightarrow$  **9**) completes the reaction.

Because of the difficulty inherent in gaining definitive information above and beyond purity and molecule symmetry from paramagnetic NMR spectra, this proposed reaction mechanism

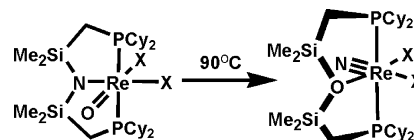


**Figure 19.** Silyl-oxo coupling in a Rhenium oxide complex on heating at  $90^\circ\text{C}$  ( $\text{X} = \text{Cl}$  or  $\text{Br}$ ).

was investigated with DFT(PBE) calculations with geometry optimization using the full ligand set. The calculations find all species in Figure 17 to be minima and with energies viable for being intermediates, whereas forming the observed product is highly exothermic. The formation of the postulated transient nitride  $[\text{PNPCoN}]^+$  and  $\text{N}_2$  from  $[\text{PNPCoN}_3]^+$  is energetically downhill by  $7.6 \text{ kcal}\cdot\text{mol}^{-1}$ ; subsequent conversion to **9** can then proceed via two energetically viable intermediates, **A** and **B**.  $[\text{PNPCoN}_3]^+$  is calculated to be a triplet ground state ( $6.5 \text{ kcal}\cdot\text{mol}^{-1}$  more stable than its singlet) as are  $\text{Co}(\text{III})$  complexes **A** and **B**; thus these are viable candidates for the three spectroscopically observed complexes.  $[\text{PNPCoN}]^+$  is calculated to be a ground-state singlet (by  $9.5 \text{ kcal}\cdot\text{mol}^{-1}$  compared to its triplet isomer); therefore, it would have to be extremely short-lived (undetectable by NMR) if present in the conversion of  $\text{PNPCoN}_3$  to **9**. The LUMO and LUMO + 1 of singlet  $[\text{PNPCoN}]^+$  (Figure 18) are primarily nitride  $p_\pi$  orbitals and thus are consistent with the nucleophile/electrophile character for P/N bond formation proposed early in Figure 17. Indeed, the LUMOs provide evidence that writing  $\text{N}^{3-}$  is an oversimplification, and thus  $[\text{CoN}]^{2+}$  is a unit where  $\text{Co}(\text{V})$  is also an imperfect description; the oxidation is borne by both nitrogen and cobalt.

From this tentative analysis, the key points that emerge are (a) an (outer sphere) oxidative event is needed to trigger  $\text{N}_2$  loss from  $(\text{PNP})\text{Co}(\text{N}_3)$ , (b) the terminal nitrogen ligand in  $[\text{PNPCoN}]^+$  is electrophilic, (c) oxidation of phosphorus to  $\text{P}(\text{V})$  is the key to subsequent bond making/breaking because it enables heterolysis of the  $\text{Si}-\text{CH}_2$  bond in the PNP backbone, and (d) the overall two-electron redox transfer again occurs at phosphorus, not cobalt. The reaction is essentially complete by



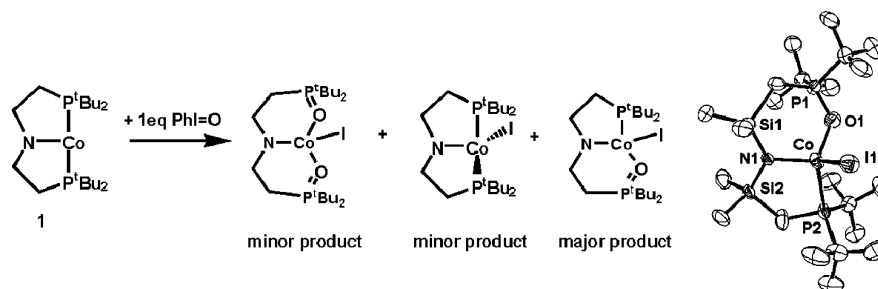


**Figure 20.** Left, the three products from the reaction of **1** with 1 equiv of PhI=O. Right, ORTEP view (50% probabilities) of **10** (hydrogens omitted for clarity). Selected bond lengths (Å) and angles (°): Co–I1, 2.5942(9); Co–P2, 2.3935(15); Co–N1, 1.952(4); Co–O1, 1.943(4); P1–O1, 1.492(4); P2–Co–O1, 116.08(14); N1–Co–I1, 125.84(12); P2–Co–I1, 111.24(5), O1–Co–I1, 105.70(14).

0 °C, so all activation energies are very modest in contrast to silyl/heteroatom coupling in Fryzuk's niobium nitride complex<sup>55</sup> (requires heating to 110 °C) and PNPreX<sub>2</sub>(O) (90 °C, Figure 19),<sup>56</sup> which have substantially higher energetic barriers.

**e. Other Oxo-Transfer Reagents.** Disappointing results of the reactivity of PNPCo with O<sub>2</sub> are described in the Supporting Information. Seeking a more controlled method for the addition of one oxygen atom to **1** (seeking a cleaner reaction), the addition of oxygen atom donors to **1** was investigated. Addition of 1 equiv of iodosobenzene, PhI=O, to a toluene solution of **1** resulted, after 18 h, in the production of three new paramagnetic products. The two minor components are readily identifiable<sup>1</sup> as the Co(II) complexes PNP(O)CoI and P(O)NP(O)CoI. The major product from this reaction possessed C<sub>s</sub> symmetry and was isolated spectroscopically pure by recrystallization from minimum (Me<sub>3</sub>Si)<sub>2</sub>O. The solid-state structure (Figure 20) revealed the insertion of an oxygen atom into a P–Co bond; along with the formation of a Co–I bond; therefore, oxidation to P(V) and Co(II) has occurred.

The structural metrics for PNP(O)CoI, **10**, are unremarkable, with P–O, O–Co and Co–I bond lengths as expected and comparable to the analogous bonds in PNP(O)CoI and [κ<sup>2</sup>-(*t*-Bu<sub>2</sub>P(I)CH<sub>2</sub>SiMe<sub>2</sub>NSiMe<sub>2</sub>CH<sub>2</sub>P<sup>t</sup>Bu<sub>2</sub>)CoI<sub>2</sub>]. There is a minor distortion in the geometry around cobalt away from ideal tetrahedral geometry, but this is attributable to the constraints imposed by the fused five- and six-membered rings. A mechanism leading to **10** can be envisaged where initial oxygen-atom transfer would generate PNP(O)Co=O, analogous to the cobalt–imido complex PNP(O)Co(NPh) that could equally undergo nucleophilic phosphine attack at an electrophilic oxygen (with numerous examples of electrophilic oxo functionalities reported). This raises the phosphorus oxidation state to five and returns cobalt to its +1 state where it then abstracts an iodide from the phenyl iodide byproduct to generate **10**. It is noteworthy that there is no oxygen–silicon bond formation in this reaction in direct contrast to the silyl–heteroatom coupling observed from the nitride analog. An intramolecular conversion analogous to that producing **9** would be expected to be kinetically faster than the bimolecular reaction involving phenyl iodide, precluding this explanation as the origin of the differing reactivity of nitride versus oxide. The relatively weaker nucleophilicity of a P=O moiety bound to cobalt when compared to the negatively charged P=N<sup>−</sup> may account for this distinct behavior. The formation of P(O)NP(O)CoI in this reaction could proceed via **10** or an undetected double oxo inserted complex, P(O)NP(O)-

Co(I). The reaction of **1** with 2 equiv of PhI=O led to the formation of P(O)NP(O)CoI<sup>1</sup> as the sole product (by <sup>1</sup>H NMR). Because of the slow nature of this heterogeneous reaction, it was not possible to use low-temperature NMR spectroscopy to probe for any reaction intermediates.

A number of other oxygen atom donors were employed, targeting the Co(I)-inserted complexes analogous to **8**. Addition of 1 equiv of either N<sub>2</sub>O or Me<sub>3</sub>NO to **1** led to one new paramagnetic complex with solution C<sub>s</sub> symmetry; **1** was still present in significant quantity. Increasing the stoichiometry of the oxygen atom donor to 3 equiv resulted in the complete consumption of **1** and an identical C<sub>s</sub> symmetric product. The oxidizing reagent independence suggests the addition of only the three oxygen atoms (i.e., Me<sub>3</sub>N and N<sub>2</sub> are innocent byproducts). The final location of the third oxygen atom is of more interest, but unfortunately, despite repeated attempts, crystals suitable for X-ray diffraction were not obtainable, frustrating definitive characterization. The mass spectrum of this compound was unhelpful, with a peak observed at 715.4 *m/z*, which we cannot assign to any expected product. Addition of an excess of N<sub>2</sub>O led to an intractable mixture of paramagnetic and diamagnetic complexes, even at −65 °C. Whereas characterization of this complex has eluded us, it is again possible to make the generic observation that oxidation of the phosphine probably occurs in preference to the cobalt center – a common theme in this work.

## Conclusions

Attempts to reach stable Co(III) complexes ligated by PNP met, counter-intuitively, with limited success; simple logic dictates that the superior electron-donating phosphine with <sup>t</sup>Bu substituents (compared to the phenyl derivative of Fryzuk)<sup>57</sup> should allow greater stabilization of this higher oxidation state. Experimentally, the opposite was ascertained, with PNP(O)CoX<sub>2</sub> complexes proving elusive; they are obtainable only when ligated with low-electronegativity ligands (hydrides/silanes), where the oxidation state formalism has less meaning. This behavior may in part be attributable to ligand noninnocence, with the presence of readily oxidized <sup>t</sup>Bu phosphines that result in phosphorus repeatedly being the locus of oxidation. The inability to access persistent PNP(O)Co=E complexes (where cobalt would equally be in the +3 oxidation state) can, in addition to the reducing power of the electron-rich PNP ligand, be attributed to weak cobalt/E bonds, with the calculated triplet ground states for four-coordinate Co(III) resulting in partially filled d orbitals

(56) Ozerov, O. V.; Gerard, H. F.; Watson, L. A.; Huffman, J. C.; Caulton, K. G. *Inorg. Chem.* **2002**, *41*, 5615.

(57) Fryzuk, M. D.; Leznoff, D. B.; Thompson, R. C.; Rettig, S. J. *J. Am. Chem. Soc.* **1998**, *120*, 10126.



that prevent the significant multiple bond cobalt–E character. Calculations and reactivity studies have shown electrophilic character for E in these cases, rendering it susceptible to rapid attack by the nucleophilic (and labile) phosphine. Thus, the overall products from the addition of electrophilic reagents (e.g.,  $\text{PhI}=\text{O}$ ,  $\text{RN}_3$ ) contain pentavalent phosphorus with the initial cobalt oxidation state unchanged. An unusual oxidative triggering of  $\text{N}_2$  elimination from 1e-oxidized  $(\text{PNP})\text{Co}(\text{N}_3)^+$  executes an even more massive ligand rearrangement, with the postulated nitride product  $(\text{PNP})\text{CoN}^+$  breaking the  $\text{Si}-\text{CH}_2$  bond to form  $\text{Si}-\text{N}$  and  $\text{N}-\text{P}$  bonds. Given the large number of thermally stable azide complexes, the oxidative triggering of  $\text{N}_2$  elimination warrants more general evaluation as a new synthetic route to metal nitrides. The new bonds formed and the final metal oxidation state show that, contrary to a redox assignment of  $(\text{PNP})\text{Co}(\text{V})(\text{N}^{3-})^+$ , the nitride is electrophilic. A related silyl–heteroatom coupling is also observed in the reaction of  $\text{PNPCo}$  with excess  $\text{PhSiH}_3$ , highlighting the fact that the amide nitrogen in PNP is not only a potent  $\pi$  donor to a metal but also it can be a reactive functionality.

The cobalt center in  $\text{PNPCo}$  was found to be extremely electron rich (by IR spectroscopy of its monocarbonyl<sup>6</sup>); in comparison to other pincer ligands, PNP builds the most reducing power into (pincer) $\text{M}$ , yielding dihydride  $\text{PNPCo}^{\text{III}}(\text{H})_2$ , not dihydrogen. The redox properties of the electron-rich  $\text{PNPCo}$  are however paradoxical; whereas one-electron oxidation of cobalt readily occurred, there was a reluctance for full two-electron transfer that would result in  $\text{Co}(\text{III})$ . To a degree, this failure (and the related inability to produce  $\text{PNPCoH}$  from reaction with hydrogen-atom donors) is due to the fact that the reducing power of  $\text{PNPCo}$  is strongly dependent on not only the redox potential of cobalt but also, equally importantly, on the energy recouped in the formation of new  $\text{Co}-\text{X}$  bonds.

Because the silylene is an electrophile, the  $\text{P}/\text{Si}$  bond formation there also exemplifies what must be  $\text{Co}/\text{P}$  bond lability when the metal oxidation state rises. At the same time, it is the apparent lability of these phosphorus on high-valent cobalt that facilitates intramolecular redox chemistry between an electrophilic ligand and  $\text{P}(\text{III})$  because the reactions observed here are not evident in PNP complexes of the less-labile  $\text{Ru}-\text{P}$  and  $\text{Os}-\text{P}$  bonds. For example, isoelectronic  $(\text{PNP})\text{RuN}$  shows<sup>52</sup> none of the chemistry found here for  $(\text{PNP})\text{CoN}^+$ , apparently due to the labile  $\text{P}/\text{Co}(\text{V})$  bond.

Overall, this work with  $\text{O}_2$ ,  $\text{I}_2$ ,  $\text{PhN}_3$ , and even  $\text{PhSiH}_3$  highlights a current common theme, that of ligand noninnocence, which in the  $\text{tBuPNP}$  ligand set is evident at both the labile, oxidizable phosphine functionalities and at the amide nitrogen with its propensity for silyl–heteroatom coupling; these ligand vulnerabilities need to be considered when attempting to install any further reactive functionality at the metal center in high oxidation state complexes with electrophilic ligands (e.g., oxo, imido, etc). Every ligand has its characteristic vulnerability,<sup>58–62</sup>

which either must be frustrated (4d and 5d metals) by kinetic inertness, or accommodated, by focusing (with PNP) on reducing reaction conditions.

## Experimental Section

**General Considerations.** All of the manipulations were performed using standard Schlenk techniques or in an argon-filled glovebox. Solvents were distilled from sodium/benzophenone,  $\text{CaH}_2$ , or 4 Å molecular sieves, degassed prior to use, and stored in airtight vessels. All of the reagents were used as received from commercial vendors or synthesized by published routes.  $\text{PNPMgCl-dioxane}$  ( $\text{PNP} = [(\text{tBuPCH}_2\text{SiMe}_2)_2\text{N}]^-$ ) and  $\text{PNPCo}$  were prepared according to literature methods.<sup>1</sup>  $^1\text{H}$  NMR chemical shifts are reported in ppm relative to protio impurities in the deuterated solvents.  $^{31}\text{P}\{^1\text{H}\}$  spectra are referenced to external standards of 85%  $\text{H}_3\text{PO}_4$  (at 0 ppm),  $^{29}\text{Si}$  and  $^{29}\text{Si}\{^1\text{H}\}$  spectra are referenced to external standards of  $(\text{CH}_3)_4\text{Si}$  (at 0 ppm). NMR spectra were recorded with a Varian Gemini 900 (300 MHz  $^1\text{H}$ , 121 MHz  $^{31}\text{P}$ , 75 MHz  $^{13}\text{C}$ ), a 400 MHz Varian Unity Inova (400 MHz  $^1\text{H}$ , 162 MHz  $^{31}\text{P}$ , 101 MHz  $^{13}\text{C}$ ), or a 500 MHz Varian Inova instrument (500 MHz  $^1\text{H}$ , 99 MHz  $^{29}\text{Si}$ ). Solution magnetic moments were recorded at 25 °C (unless otherwise stated) using the Evans method.<sup>63,64</sup> Consistently for these paramagnetic complexes, no  $^{31}\text{P}\{^1\text{H}\}$  was observable. Infrared spectra were recorded on a Nicolet 510P FTIR spectrometer.

**$\text{PNPCoGalvinoxyl}$  (2). Method A.** A Schlenk flask was charged with  $\text{PNPCoNH}(2,6\text{-Me}_2\text{-C}_6\text{H}_3)$  (0.055 g, 0.087 mmol) and 5 mL of toluene to yield a dark-purple solution. One equiv of galvinoxyl free radical (0.037 g, 0.087 mmol) was dissolved in 5 mL toluene and added dropwise over the course of 5 min. This resulted in an immediate color change from purple to vermillion, and the solution was stirred for a further 15 min. The solvent was then removed in vacuo, and the red oil was redissolved in a minimum volume of pentane, and red crystals (0.032 g, 0.035 mmol) suitable for an X-ray diffraction study were formed on storing at  $-40$  °C for 18 h.

**Method B.** A J. Young NMR tube was charged with  $\text{PNPCo}$  (0.010 g, 0.02 mmol) and 0.45 mL of  $\text{C}_6\text{D}_6$ , and the addition of 1 equiv of galvinoxyl free radical as a solid (0.008 g, 0.02 mmol) resulted in a rapid color change from green to red and NMR spectra identical to that observed from Method A, indicating the formation of  $\text{PNPCoGalvinoxyl}$ . Yield (from Method A): 40% (quantitative by NMR).  $^1\text{H}$  NMR (298 K,  $\text{C}_6\text{D}_6$ ): 69.84 (broad singlet, 4H), 44.15 (sharp singlet overlapped with a broad singlet, combined intensity of region = 14H), 22.6 (s, 2H), 16.02 (s, 1H), 3.80 (18H, s), 2.85 (s, 18H),  $-13.82$  (br s, 36H). Magnetic Moment ( $\text{C}_6\text{D}_6$ ):  $\mu_{\text{eff}} = 3.94\mu_{\text{B}}$ . IR ( $\text{cm}^{-1}$ , pentane)  $\text{C}=\text{O}$  quinone stretch: 1610. Mass spec. (ESI<sup>+</sup>): Calcd. (for  $\text{C}_{51}\text{H}_{93}\text{CoNO}_2\text{P}_2\text{Si}_2$ ): 928.6, Found: 928.8.

**$\text{PNPCo}(\text{H})_2$  (3).** In a standard experiment, a J. Young NMR tube was charged with  $\text{PNPCo}$  (0.09 g, 0.04 mmol) and dissolved in 0.45 mL of  $\text{C}_6\text{D}_6$ . On a gas line, the green solution was degassed three times by freeze/pump/thaw cycles and charged with  $\text{H}_2$  at 77 K (ca. 4 atm). On thawing, this yielded an immediate color change to a yellow/brown solution. The integration of the hydride region was performed against the backbone, intensity 4,  $\text{CH}_2$  resonance at 0.92 ppm, and is

(58) Fekl, U.; Goldberg, K. I. *J. Am. Chem. Soc.* **2002**, *124*, 6804.

(59) Kuhlman, R.; Streib, K.; Caulton, K. G. *J. Am. Chem. Soc.* **1993**, *115*, 5813.

(60) Blackmore, I. J.; Gibson, V. C.; Hitchcock, P. B.; Rees, C. W.; Williams, D. J.; White, A. J. P. *J. Am. Chem. Soc.* **2005**, *127*, 6012.

(61) Bartos, M. J.; Gordon-Wylie, S. W.; Fox, B. G.; James Wright, L.; Weintraub, S. T.; Kauffmann, K. E.; Munck, E.; Kostka, K. L.; Uffelman, E. S.; Rickard, C. E. F.; Noon, K. R.; Collins, T. J. *Coord. Chem. Rev.* **1998**, *174*, 361.

(62) Reardon, D.; Conan, F.; Gambarotta, S.; Yap, G.; Wang, Q. *J. Am. Chem. Soc.* **1999**, *121*, 9318.

(63) Evans, D. F. *J. Chem. Soc.* **1959**, 2003.

(64) Sur, S. K. *J. Magn. Reson.* **1989**, *82*, 169.

consistently of 2H intensity (with a  $d1 = 10$  s). <sup>1</sup>H NMR (298K, C<sub>6</sub>D<sub>6</sub>): 1.26 (br s, 36H), 0.93 (br s, 4H) 0.39 (br s, 12H) and −32.2 (t,  $J_{P-H}$  51 Hz, 2H). <sup>1</sup>H{<sup>31</sup>P} NMR (298 K, C<sub>6</sub>D<sub>6</sub>): 1.25 (s, 36H), 0.91 (s, 4H), 0.40 (s, 12H), and −32.2 (s, 2H) <sup>31</sup>P-{<sup>1</sup>H} NMR (298K, C<sub>6</sub>D<sub>6</sub>): 89.9 (very broad singlet).

{ $\kappa^2$ -Bu<sub>2</sub>PCH<sub>2</sub>Me<sub>2</sub>SiNSiMe<sub>2</sub>CH<sub>2</sub>'Bu<sub>2</sub>P(H)Si= }Co(H)<sub>3</sub>-(SiH<sub>2</sub>Ph)<sub>2</sub> (**4**). A Schlenk flask was charged with PNPCo (0.100 g, 0.2 mmol) and dissolved in 10 mL of toluene. PhSiH<sub>3</sub> (4.1 equiv, 0.087 g, 0.81 mmol) was then added dropwise at 25 °C while stirring; an immediate color change to brown was observed followed rapidly by a second color change to pale yellow. The solvent was then removed in vacuo to yield a pale-yellow oil. Conversion to **4** was quantitative by NMR spectroscopy. This oil was dissolved in a 50/50 mix of pentane and (CH<sub>3</sub>)<sub>4</sub>Si, and the solvent was allowed to slowly evaporate, yielding a number of pale-yellow crystals suitable for X-ray diffraction. The NMR spectra (below) of these crystals (apart from resonances associated with Ph<sub>2</sub>SiH<sub>2</sub>) were identical to those observed for the isolated oil. Attempts at large-scale recrystallization repeatedly failed in part due to the thermal sensitivity of **4** (**4** was not observable by NMR after 15 h in benzene at 25 °C), producing an intractable unidentified mixture. The integration of the <sup>1</sup>H NMR was performed with a  $d1 = 10$  s to ensure full relaxation. A number of the CH<sub>2</sub> resonances in the <sup>1</sup>H and <sup>1</sup>H{<sup>31</sup>P} are obscured making a complete assignment of all inequivalent proton environments impossible. Yield: Quantitative by NMR. <sup>1</sup>H NMR (298 K, C<sub>6</sub>D<sub>6</sub>): 8.9–8.00 (m, 4H, Ph) 7.30–7.22 (m, 6H, Ph), 5.93 (d,  $J_{P-H}$  50 Hz Silylene Si–H), 5.75 (br s, 1H, Si–H), 5.70 (br s, 1H, Si–H), 5.54 (br s, 1H, Si–H) 5.31 (br s, Si–H), 1.32–0.92 (4 doublets at 1.32, 1.24, 1.01, and 0.96 all with  $J_{P-H} = 12$  Hz for the four inequivalent 'Bu groups overlapped with unresolved multiplets for the four inequivalent CH<sub>2</sub> protons, combined intensity of region = 40H), 0.30 (s, 3H Si–Me), 0.27 (s, 3H, Si–Me), 0.26 (s, 3H, Si–Me), 0.23 (s, 3H, Si–Me), and −11.29 (s, 3H Co–H). <sup>1</sup>H{<sup>31</sup>P} NMR (298 K, C<sub>6</sub>D<sub>6</sub>): 8.16–8.01 (m, 4H, Ph), 7.31–7.21 (m, 6H, Ph), 5.93 (s, 1H, silylene Si–H), 5.74 (br s, 1H, Si–H), 5.69 (br s, 1H, Si–H), 5.53 (br s, 1H, Si–H), 5.31 (br s, 1H, Si–H), 1.32–0.95 (four singlets for overlapped with unresolved multiplets for the four inequivalent CH<sub>2</sub>, combined intensity of region = 40H), 0.30 (s, 3H, Si–Me), 0.26 (s, 6H, 2 co-incident Si–Me), 0.23 (s, 3H, Si–Me), and −11.29 (s, 3H, Co–H). <sup>31</sup>P{<sup>1</sup>H} NMR (298 K, C<sub>6</sub>D<sub>6</sub>): 82.3 (br s) and 25.6 (d,  $J_{P-P}$  16 Hz). <sup>29</sup>Si NMR (280 K, C<sub>6</sub>D<sub>6</sub>): 34.0 (d, 158 Hz), 9.1 (s), 2.6 (s), −15.2 (t, 168 Hz), −29.6 (t, 168 Hz). <sup>29</sup>Si{<sup>1</sup>H} NMR (280 K, C<sub>6</sub>D<sub>6</sub>): 33.2 (s), 8.2 (s), 1.7 (s), −16.0 (s), −30.1 (s). Ph<sub>2</sub>SiH<sub>2</sub>: <sup>29</sup>Si NMR (298 K C<sub>6</sub>D<sub>6</sub>): −34.0 (t,  $J_{Si-H} = 90$  Hz). <sup>29</sup>Si{<sup>1</sup>H} NMR (298 K C<sub>6</sub>D<sub>6</sub>): −34.0 (s). <sup>1</sup>H NMR selected (298 K, C<sub>6</sub>D<sub>6</sub>): 5.07 (s, Si–H).

{ $\kappa^2$ -Bu<sub>2</sub>PCH<sub>2</sub>Me<sub>2</sub>SiNSiMe<sub>2</sub>CH<sub>2</sub>'Bu<sub>2</sub>P(H)Si= }Co(H)<sub>4</sub>-(SiHPh)<sub>2</sub> (**5**). A Schlenk flask was charged with PNPCo (0.09 g, 0.04 mmol) and dissolved in 5 mL of toluene, resulting in a green solution. The solution was then cooled to −78 °C and 2 equiv of PhSiH<sub>3</sub> (0.009 g, 0.08 mmol) was added by syringe while stirring, resulting in an immediate color change to brown. The solvent was then removed in vacuo to yield **5** quantitatively (by NMR) as a brown oil. Attempts to produce a crystalline solid repeatedly failed in part due to its thermal instability (no **5** remains after 6 h at 25 °C in benzene, producing an intractable unidentified mixture). Yield: Quantitative by NMR spectroscopy.

<sup>1</sup>H NMR (298 K, d<sub>8</sub>-toluene): 8.07–8.00 (4H, m, Ph) 7.51–7.9 (6H, m, Ph), 6.32 (1H, s, Si–H), 5.99 (d,  $J_{P-H}$  49 Hz silylene Si–H), 1.22–0.87 (40H, overlapping signals for four inequivalent 'Bu and four inequivalent CH<sub>2</sub>), 0.28 (3H, s, Si–Me), 0.24 (6H, s, 2 Si–Me co-incident), 0.9 (3H, s, Si–Me) and −11.46 (4H, s, Co–H). <sup>1</sup>H{<sup>31</sup>P} NMR (298 K, d<sub>8</sub>-toluene): 8.06–8.00 (4H, m, Ph), 7.48–7.19 (6H, m, Ph), 6.32 (s, 1H Si–H), 6.00 (s, 1H, Silylene Si–H), 1.9–0.89 (40H, 'Bu and CH<sub>2</sub> resonances), −11.43 (s, 4H, Co–H). <sup>31</sup>P{<sup>1</sup>H} NMR (298 K, d<sub>8</sub>-toluene): 92.7 (br, s) and 19.2 (d,  $J_{P-P}$  19 Hz). <sup>29</sup>Si NMR (263 K, d<sub>8</sub>-toluene): 22.2 (d,  $J_{Si-H}$  162 Hz), 10.0 (s), 2.7 (s), −18.9 (d,  $J_{Si-H}$  195 Hz). <sup>29</sup>Si{<sup>1</sup>H} NMR (263 K, d<sub>8</sub>-toluene): 22.3 (s), 9.9 (s), 2.6 (s), −18.8 (s).

**PNPCoN<sub>2</sub>C(H)SiMe<sub>3</sub> (**6**).** A Schlenk flask was charged with PNPCo (0.050 g, 0.1 mmol) and dissolved in 5 mL of toluene. To this green solution was added 1 equiv of N<sub>2</sub>C(H)SiMe<sub>3</sub> as a 2 M ether solution (50 μL, 0.1 mmol), resulting in an immediate color change to dark yellow. The toluene was removed in vacuo, and the resultant dark-yellow oil redissolved in (Me<sub>3</sub>Si)<sub>2</sub>O and was stored at −40 °C for 18 h to yield dark-yellow crystals (0.019 g, 0.03 mmol). Yield: 31% (the conversion was quantitative by NMR). <sup>1</sup>H NMR (298 K, C<sub>6</sub>D<sub>6</sub>): 1.35 (36H br s), 0.68 (4H, br s), 0.6 (21H br s), −3.04 (1H, br s). <sup>31</sup>P{<sup>1</sup>H} NMR (298 K C<sub>6</sub>D<sub>6</sub>): 52.3 (br s). <sup>13</sup>C{<sup>1</sup>H} NMR (298 K C<sub>6</sub>D<sub>6</sub>): 33.4 (br s), 29.7 (br s), 8.7 (br s), 6.4 (br s), 1.1 (br s), despite numerous attempts, the diazoalkane carbon was not observed in range +400 to −90 ppm. IR (cm<sup>−1</sup>, pentane): 2069.

**PNPCoN<sub>2</sub>C(H)Ph (**7**).** Synthesized in an entirely analogous manner to PNPCoN<sub>2</sub>C(H)SiMe<sub>3</sub> although solid material could not be obtained despite repeated attempts. The conversion was quantitative by <sup>1</sup>H NMR spectroscopy. <sup>1</sup>H NMR (298 K, C<sub>6</sub>D<sub>6</sub>): 7.41 (1H, m), 6.99 (2H, m), 6.58 (2H, m), 1.26 (36H, br s), 0.76 (4H, br s), 0.14 (12H br s), −0.83 (1H, br s). <sup>31</sup>P-{<sup>1</sup>H} NMR (298 K C<sub>6</sub>D<sub>6</sub>): 48.5 (br s). <sup>13</sup>C{<sup>1</sup>H} NMR (298 K C<sub>6</sub>D<sub>6</sub>): 161.9 (s), 136.6 (s), 19.7 (s), 118.7 (s), 41.5 (br s), 33.5 (s), 29.4 (s), 8.2 (s), 6.2 (s). IR (cm<sup>−1</sup>, pentane): 1592.

**PNP(P=NPh)Co (**8**).** A Schlenk flask was charged with PNPCo (0.123 g, 0.23 mmol) and 10 mL of pentane and cooled to −78 °C; at this temperature a solution of PhN<sub>3</sub> (31 μL, 0.23 mmol) dissolved in 5 mL of pentane was added dropwise over the course of 10 min. This resulted in a rapid color change from green to brown. The solution was stirred for a further 10 min at this temperature before being allowed to warm to 25 °C. The pentane was reduced to a minimum volume and stored at −40 °C for 1 day to yield dark-yellow crystals (0.063 g). After isolation of the first crop of crystals, the supernatant was reduced in volume further and cooled to −40 °C for 18 h to yield a second crop (0.016 g) of crystals. A final crop (0.018 g) can be obtained by slow evaporation of the remaining pentane solvent followed by washing with cold pentane, to give a combined quantity of 0.097 g (0.16 mmol). Yield: 70%. <sup>1</sup>H NMR (298 K, C<sub>6</sub>D<sub>6</sub>): 24.27 (s, 2H), 10.96 (s, 18H), 8.64 (s, 18H), 6.70 (s, 2H), 0.27 (s, 6H), −4.16 (s, 6H), −35.14 (br s, 2H), −39.27 (s, 1H), −40.30 (s, 2H). <sup>31</sup>P{<sup>1</sup>H} NMR (298 K, C<sub>6</sub>D<sub>6</sub>): 206.8. <sup>13</sup>C{<sup>1</sup>H} NMR (298 K, C<sub>6</sub>D<sub>6</sub>): 502.0 (br s), 461.7 (br s), 402.9 (br s), 338.4 (br s), 186.5 (s), 157.9 (br s), 147.7 (br s), 8.8 (s), −31.3 (br s), −56.1 (s), −99.7 (s), −237.9 (br s). Magnetic Moment (C<sub>6</sub>D<sub>6</sub>):  $\mu_{\text{eff}} = 3.40\mu_B$ .

**Low-Temperature NMR Analysis on PNPCo + 0.90 equiv of PhN<sub>3</sub>.** A Young NMR tube was charged with PNPCo (0.09

g, 0.04 mmol) and dissolved in 0.30 mL of  $d_8$ -toluene and then cooled to  $-78^\circ\text{C}$ . A solution of  $\text{PhN}_3$  (5  $\mu\text{L}$ , 0.038 mmol) dissolved in 0.2 mL of  $d_8$ -toluene was cooled to  $-78^\circ\text{C}$  and added dropwise to the cooled solution of  $\text{PNPCo}$ . The tube was then sealed and carefully agitated, to ensure no solvent warming; this resulted in a brown solution.  $^1\text{H}$  NMR (213 K,  $\text{C}_7\text{D}_8$ ): 1.26 (36H, br s), 0.78 (4H, br s), 0.05 (12H, br s); phenyl region was not clearly resolved.  $^{31}\text{P}\{^1\text{H}\}$  NMR (213 K  $\text{C}_7\text{D}_8$ ): 53.95 (s).

On warming to  $-40^\circ\text{C}$  the first change in the NMR spectra was observed, with the diamagnetic signals gradually disappearing over the course of 30 min; concomitantly, new paramagnetic signals were then observed. In addition, the sample at this temperature was now a dark green.  $^1\text{H}$  NMR (233 K,  $\text{C}_7\text{D}_8$ ): 7.2 (v. br s overlapped with protio toluene signals preventing accurate integration), 0.3 (4H, br s),  $-2.1$  (12H, br s).  $^{31}\text{P}\{^1\text{H}\}$  NMR (233 K  $\text{C}_7\text{D}_8$ ): No phosphorus resonances was observed from  $+400$  to  $-300$  ppm.

At  $-20^\circ\text{C}$ , the  $\text{C}_{2v}$  paramagnetic product decreased in intensity with peaks attributable to  $\text{PN}(\text{P}=\text{NPh})\text{Co}$  growing in. At  $-20^\circ\text{C}$ , the conversion to  $\text{PN}(\text{P}=\text{NPh})\text{Co}$  was complete after 10 min and the solution now was a dark yellow.

**$[\text{PNNP}=\text{CH}_2\text{Co}][\text{Y}]$  (9).**  **$[\text{PNNP}=\text{CH}_2\text{Co}] = [\text{Bu}_2\text{PCH}_2\text{Si}(\text{Me})_2\text{NSi}(\text{Me})_2\text{NP}(\text{Bu}_2)=\text{CH}_2\text{Co}]$ .**  **$[\text{Y}] = [\text{PF}_6]$ .** A Schlenk flask was charged with  $\text{PNPCoN}_3$  (0.030 g, 0.05 mmol) and dissolved in 5 mL of THF.  $\text{Cp}_2\text{FePF}_6$  (0.95 equiv, 0.016 g, 0.05 mmol) was then added as a solid and stirred overnight. The solution changes from a red/brown to a red over the course of the reaction. The solvent was then removed in vacuo, and the resultant oil was washed with pentane ( $2 \times 5$  mL portions). The oil was then dried in vacuo, redissolved in minimum THF, and cooled to  $-40^\circ\text{C}$  overnight to yield red needles (0.021 g) (crystals suitable for X-ray diffraction study formed spontaneously in a Young NMR tube charged with 0.09 g of  $\text{PNPCoN}_3$ , 0.0075 g of  $\text{Cp}_2\text{FePF}_6$ , and 0.4 mL of  $d_8$ -THF and rotated overnight). Yield: 58%.  $^1\text{H}$  NMR (298 K,  $d_8$ -THF): 33.14 (s, 6H), 7.62 (s, 6H),  $-1.11$  (s, 18H),  $-12.71$  (s, 18H),  $-15.47$  (s, 2H). The  $\text{P}=\text{CH}_2$  protons are not observed presumably due to their proximity to paramagnetic cobalt.  $^{31}\text{P}\{^1\text{H}\}$  NMR (298 K,

$d_8$ -THF):  $-140.6$  (septet,  $J_{\text{P-F}} = 712$  Hz).  $^{19}\text{F}\{^1\text{H}\}$  NMR (298 K,  $d_8$ -THF):  $-67.9$  (d,  $J_{\text{F-P}} = 712$  Hz). Magnetic moment ( $d_8$ -THF, 298 K):  $\mu_{\text{eff}} = 3.0\mu_{\text{B}}$ . Mass spec (ESI+,  $m/z$ ): Calcd. for  $\text{C}_{22}\text{H}_{52}\text{CoN}_2\text{P}_2\text{Si}_2$ : 521.25, Found: 521.2.

**$[\text{Y}] = [\text{BAr}_\text{F}]$  ( $\text{BAr}_\text{F} = [\text{B}\{3,5\text{-C}_6\text{H}_3(\text{CF}_3)_2\}_4]$ ).** In a standard reaction, a Young NMR tube was charged with  $\text{PNPCoN}_3$  (0.015 g, 0.026 mmol),  $\text{Cp}_2\text{FeBAr}_\text{F}$  (0.028 g, 0.026 mmol), and 0.45 mL of  $d_8$ -THF was added. Immediate gas evolution was observed, and the resultant solution was deep red. The  $^1\text{H}$  NMR reveals one cobalt-containing product along with a singlet attributable to  $\text{Cp}_2\text{Fe}$ . Attempts to obtain crystalline material of this complex repeatedly failed, even at a larger scale.  $^1\text{H}$  NMR (298 K,  $d_8$ -THF): 33.36 (s, 6H), 7.73 (14H, s, overlap of aromatic C–H with Si–Me), 7.52 (s, 4H),  $-1.01$  (s, 18H),  $-12.84$  (s, 18H),  $-15.54$  (s, 2H).  $^{19}\text{F}\{^1\text{H}\}$  (298 K,  $d_8$ -THF):  $-60.3$  (s).  $^1\text{H}$  NMR (288 K,  $d_8$ -THF): 35.76 (s, 6H), 8.6 (s, 6H), 7.72 (s, 8H), 7.52 (s, 4H),  $-1.16$  (s, 18H),  $-13.84$  (s, 18H),  $-15.70$  (s, 2H).

**$\text{PN}(\text{P}=\text{O})\text{CoI}$  (10).** A Schlenk flask was charged with  $\text{PNPCo}$  (0.040 g, 0.08 mmol) and dissolved in 5 mL of toluene; one equivalent of  $\text{PhI}=\text{O}$  (0.06 g, 0.08 mmol) was added as a solid and the stirred for 18 h. This resulted in the gradual dissolution of  $\text{PhI}=\text{O}$  and a color change from green to blue. Removal of toluene in vacuo resulted in a blue oil. Recrystallization from minimum  $(\text{Me}_3\text{Si})_2\text{O}$  at  $-40^\circ\text{C}$  yielded blue crystals (0.014 g, 0.021 mmol) that were suitable for an X-ray diffraction study. Isolated Yield: 27%.  $^1\text{H}$  NMR ( $\text{C}_6\text{D}_6$ , 298 K): 43.31 (6H, br s), 23.40 (2H, br s), 18.94 (2H, br s), 4.44 (18H, br s),  $-8.58$  (18H, br s), and  $-36.57$  (6H, br s). Magnetic Moment ( $\text{C}_6\text{D}_6$ ):  $\mu_{\text{eff}} = 4.10\mu_{\text{B}}$ .

**Acknowledgment.** This work was supported by the NSF (CHE-0544829). Professors Mu-Hyun Baik and Daniel Mindiola are thanked for useful discussions.

**Supporting Information Available:** CIF files for all crystal structures. This material is available free of charge via the Internet at <http://pubs.acs.org>.

JA074378+